Supporting Information (SI)

Advancing Energetic Chemistry: First Synthesis of Sulfur-Based C-C Bonded Thiadiazole-Pyrazine Compounds with Nitrimino Moiety

Parasar Kumar,[a] Vikas D. Ghule,[b] Srinivas Dharavath [a]*

[a]Energetic Materials Laboratory, Department of Chemistry, Indian Institute of Technology Kanpur, Kanpur-208016, Uttar Pradesh, India.

E-mail: srinivasd@iitk.ac.in

[b]Department of Chemistry, National Institute of Technology Kurukshetra, Kurukshetra-136119, Haryana, India.

Table of Contents

Caution! All the compounds investigated are potentially explosive, energetic materials. Although we have experienced no difficulties in syntheses and characterization of these compounds, manipulations must be carried out by using appropriate standard safety precautions. Eye protection and leather gloves must be always worn.

General Methods.

Reagents were purchased from Ak Scientifics, Acros Organics, or Aldrich as analytical grade and were used as received. ^{1}H NMR and ^{13}C NMR spectra were recorded using JEOL DELTA (ECS) 500 (^{1}H, 500 MHz; ^{13}C, 126 MHz) nuclear magnetic resonance spectrometer. DMSO-d_6 was employed as the solvent and locking solvent. Chemical shifts are given relative to $(CH_3)_4Si$ for ^{1}H and ^{13}C spectra. HRMS was recorded on a Quadrupole Time-of-Flight (Q-TOF) Mass Spectrometry Decomposition temperatures (onset) were recorded using a dry nitrogen gas purge and at a heating rate of 5 °C min^{-1} on a differential scanning calorimeter (SDT650). IR spectra were recorded using Zn-Se pellets with ECO-ATR spectrometer (Bruker Alpha II). Density was determined at room temperature by employing Anton Par Ultra5000 gas pycnometer in helium atmosphere. Impact and friction-sensitivity measurements were tested by employing a standard BAM Fall hammer and a BAM friction tester. The single-crystal X-ray data collection was carried out using Bruker APEX-II CCD diffractometer. The crystal was kept at 100 K during data collection.

Experimental Section:

***Synthesis of pyrazine-2,3-dicarbonitrile (1)*:** 2,3-diaminomaleonitrile (1 gm, 9.25 mmol) and glyoxal (1.52 gm, 26.2 mmol) was suspended in water (20 mL) and to this oxalic acid dihydrate (240 mg, 1.9 mmol) was added slowly with constant stirring. The reaction mixture was heated to 80 °C for 4 hours, cooled to room temperature. Newly formed precipitate was filtered off, washed with distilled water, and dried in oven at 50 °C to get pure product. The spectroscopic data were well matching with the previous literature.[1] Yield 85% (1023 mg, 7.87 mmol). ^{1}H NMR (500 MHz, $CDCl_3$): δ (ppm) 8.94 (s, 2H). ^{13}C NMR (126 MHz, $CDCl_3$): δ(ppm) 147.25, 134.18, 112.77.

***Synthesis of 5,5'-(pyrazine-2,3-diyl)bis(1,3,4-thiadiazol-2-amine) (2)*:** Compound **1** (1500 mg, 11.5 mmol) was slowly added to trifluoroacetic acid (TFA, 25 mL) followed by the pinch-wise addition of thiosemicarbazide (2625 mg, 28.84 mmol) at room temperature. The reaction mixture was heated to 60 ˚C for 16 hours and allowed to cool down to room

temperature. Aqueous ammonium solution (25%) was added dropwise to the reaction mixture till the white fume ceases and the formation of precipitate was observed. The newly formed precipitate was filtered, washed with cold water, and dried in oven at 50 ˚C to get pure brown solid in 87% yield (2790 mg, 10 mmol). T_d(onset): 252 ℃. ^{1}H NMR (500 MHz, DMSO-d_6): δ (ppm) 8.74 (s, 2H), 7.56 (s, 4H). ^{13}C NMR (126 MHz, DMSO-d_6): δ(ppm) 170.34, 154.00, 143.49, 142.74. IR (ATR, ZnSe, cm^{-1}): 867, 1071,1128, 1169, 1398, 1494, 1605, 3078, 3240. HRMS (ESI-QTOF) m/z: calculated for $C_8H_6N_8S_2$ $[M+H]^+$ 279.0230; found 279.0237.

***Synthesis of 5,5'-(pyrazine-2,3-diyl)bis(1,3,4-thiadiazol-2-nitrimino) (3)*:** 100% HNO_3 (6 mL), 98% H_2SO_4 (9 mL) was placed in ice bath and to this compound **2** (1000 mg, 3.59 mmol) was added slowly with uniform stirring. The reaction mixture was stirred at the same temperature for 30 minutes and then at room temperature for 12 hours. The brownish solution was poured into crushed ice. The formed yellow precipitate was filtered off, washed with water, and dried in oven. Yield 72% (954 mg, 2.59 mmol). T_d(onset): 207 ℃. ^{1}H NMR (500 MHz, DMSO-d_6): δ (ppm) 8.99 (s, 2H). ^{13}C NMR (126 MHz, DMSO-d_6): 171.38, 156.53, 145.40, 141.53 . IR (ATR, ZnSe, cm^{-1}): 761, 992, 1236, 1389, 1508, 1549, 2845, 2996. HRMS (ESI-QTOF) m/z: calculated for $C_8H_4N_{10}O_4S_2$ $[M-H]^-$ 366.9786; found 366.9784. Elemental analysis: (%) calculated for $C_8H_4N_{10}O_4S_2$ (368.30): C, 26.09; H, 1.09; N, 38.03; S, 17.41; found C, 26.64; H, 1.47; N, 38.02; S, 17.10.

General procedure for the synthesis of salts 4-7: Compound **3** (100 mg, 0.27 mmol) was dissolved in methanol (5 mL), to this base hydrazine monohydrate (41 mg, 0.8 mmol), hydroxylamine hydrate (41 mg, 0.8 mmol), 7*H*-[1,2,4]triazolo[4,3-b][1,2,4]triazole-3,6,7-triamine (TATOT) (88 mg, 0.57 mmol) and 3,5-diamino-4*H*-1,2,4-triazole (DAT) (59 mg, 0.59 mmol) was added and stirred at room temperature for 12 hours. The formed precipitate

was collected by filtration, washed with methanol and dried in air to obtain pure product in quantitative yield.

***Synthesis of dihydrazinium-(pyrazine-2,3-diylbis(1,3,4-thiadiazole-5,2-diyl))bis(nitroamide) (4)*:** Dark yellow. Yield 84 % (98 mg, 0.22 mmol). T_d(onset): 222 °C. ^{1}H NMR (500 MHz, DMSO-d_6): δ (ppm) 8.76 (s, 2H), 5.44 (br, 10H). ^{13}C NMR (126 MHz, DMSO-d_6): δ(ppm) 171.62, 158.16, 144.23, 143.42. IR (ATR, ZnSe, cm^{-1}): 957, 1076, 1312, 1380, 1535, 1601, 3318, 3399. Elemental analysis: (%) calculated for $C_8H_{12}N_{14}O_4S_2 \cdot 1.5H_2O$ (459.42): C, 20.92; H, 3.29; N, 42.98; S, 13.96; found C, 20.00; H, 3.52; N, 43.08; S, 13.12.

***Synthesis of dihydroxylammonium -(pyrazine-2,3-diylbis(1,3,4-thiadiazole-5,2-diyl))bis(nitroamide) (5)*:** Dark yellow. Yield 87 % (102 mg, 0.23 mmol). T_d(onset): 225 °C. ^{1}H NMR (500 MHz, DMSO-d_6): δ (ppm) 8.77 (s, 2H), 7.14 (br, 7H). ^{13}C NMR (126 MHz, DMSO-d_6): δ(ppm) 171.64, 158.23, 144.21, 143.52. IR (ATR, ZnSe, cm^{-1}): 1012, 1131, 1317, 1384, 1626, 1684, 2827, 2885, 3026. Elemental analysis: (%) calculated for $C_8H_{10}N_{12}O_6S_2$ (434.36): C, 22.12; H, 2.32; N, 38.70; S, 14.76; found C, 22.12; H, 3.52; N, 38.21; S, 14.63.

***Synthesis of di-3,6,7-triamino-7H-[1,2,4]triazolo[4,3-b][1,2,4]triazol-2-ium-(pyrazine-2,3-diylbis(1,3,4-thiadiazole-5,2-diyl))bis(nitroamide) (6)*:** Light yellow. Yield 80% (147 mg, 0.21 mmol). T_d(onset): 245 °C. ^{1}H NMR (500 MHz, DMSO-d_6): δ (ppm) 8.81(s, 2H), 8.20 (s, 4H), 7.23 (s, 4H), 5.77 (s, 4H). ^{13}C NMR (126 MHz, DMSO-d_6): δ(ppm) 171.67, 160.15, 157.80, 147.42, 143.93, 143.51, 141.12. IR (ATR, ZnSe, cm^{-1}): 842, 994, 1077, 1132, 1237, 1280, 1398, 1445, 1499, 1564, 1658, 3126, 3326, 3426. Elemental analysis: (%) calculated for $C_{14}H_{16}N_{26}O_4S_2$ (676.58): C, 24.85; H, 2.38; N, 53.83; S, 9.48; found C, 24.29; H, 2.78; N, 57.38; S, 7.09.

***Synthesis of di-3,5-diamino-4H-1,2,4-triazol-1-ium-(pyrazine-2,3-diylbis(1,3,4-thiadiazole-5,2-diyl))bis(nitroamide) (7)*:** brownish yellow. Yield 78% (120 mg, 0.21 mmol). T_d(onset): 246 °C. ^{1}H NMR (500 MHz, DMSO-d_6): δ (ppm) 8.77 (s, 2H), 7.33 (br, 4H). ^{13}C NMR (126 MHz, DMSO-d_6): δ(ppm) 171.62, 158.13, 151.86, 144.12, 143.51. IR (ATR, ZnSe, cm^{-1}): 715, 798, 999, 1076, 1350, 1454, 1671, 2660, 2975, 3117, 3326. Elemental analysis: (%) calculated for $C_{12}H_{14}N_{20}O_4S_2 \cdot 0.5H_2O$ (575.50): C, 25.04; H, 2.63; N, 48.68; S, 11.14; found C, 25.21; H, 2.65; N, 48.20; S, 10.56.

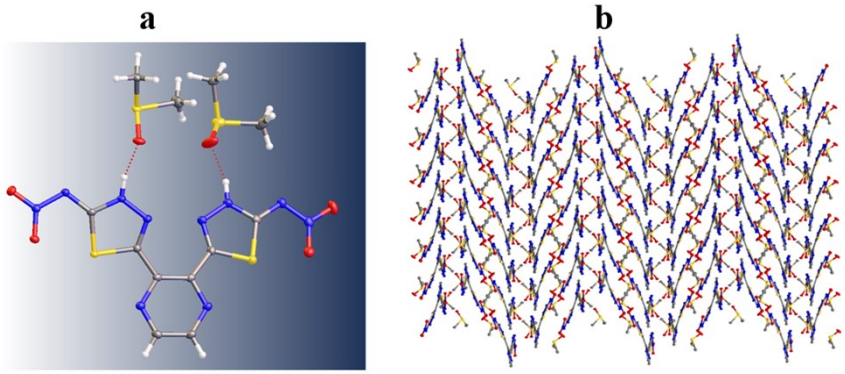

Figure S1: Crystal structure and wave-like crystal packing of **3.**

Table S1: Crystallographic data for 3.

CCDC	2379790
Empirical formula	$C_{12}H_{16}N_{10}O_6S_4$
Formula weight	524.59
Temperature/K	100
Crystal system	monoclinic
Space group	$P2_1/c$
a/Å	10.8555(4)
b/Å	20.0560(8)
c/Å	10.9976(4)
α/°	90
β/°	117.7980(10)

γ/°	90
Volume/Å3	2118.06(14)
Z	4
ρcalcg/cm3	1.645
μ/mm-1	0.504
F(000)	1080.0
Crystal size/mm3	0.2 × 0.15 × 0.1
Radiation	MoKα (λ = 0.71073)
2Θ range for data collection/°	4.062 to 56.7
Index ranges	-14 ≤ h ≤ 14, -26 ≤ k ≤ 26, -14 ≤ l ≤ 14
Reflections collected	35922
Independent reflections	5296 [Rint = 0.0464, Rsigma = 0.0296]
Data/restraints/parameters	5296/0/293
Goodness-of-fit on F2	1.053
Final R indexes [I>=2σ (I)]	R1 = 0.0355, wR2 = 0.0799
Final R indexes [all data]	R1 = 0.0449, wR2 = 0.0848
Largest diff. peak/hole / e Å-3	0.91/-0.41

Table S2: Fractional Atomic Coordinates ($\times 10^4$) and Equivalent Isotropic Displacement Parameters ($Å^2 \times 10^3$) for **3**. Ueq is defined as 1/3 of of the trace of the orthogonalised U_{IJ} tensor.

Atom	***x***	***y***	***z***	**U(eq)**
S2	-613.9(4)	6671.2(2)	3975.1(4)	13.84(10)
S002	4455.7(5)	6868.2(2)	2927.0(5)	17.23(10)
S1	4651.3(5)	5998.8(2)	10120.9(5)	15.55(10)
S004	7009.8(6)	4740.3(3)	6537.7(6)	26.12(12)
O005	-2289.3(13)	6894.4(7)	1423.5(13)	18.0(3)
O006	-1863.6(14)	6901.6(7)	-323.2(13)	21.5(3)
O007	3696.7(14)	7279.3(7)	3533.8(15)	21.4(3)
O008	6805.4(15)	5548.2(7)	12182.8(14)	23.0(3)
O009	8743.2(15)	5166.0(8)	12320.4(15)	27.2(3)
N4	1685.0(16)	6856.5(8)	3967.3(15)	15.0(3)
N2	1922.3(17)	6413.3(8)	9219.9(16)	16.5(3)
N6	-1465.4(16)	6885.3(8)	925.5(16)	15.0(3)
N8	5249.4(16)	5750.6(8)	8210.2(16)	17.4(3)
N5	-69.9(16)	6863.5(8)	1739.9(15)	14.7(3)
N1	-331.7(16)	6603.8(8)	6657.9(16)	16.3(3)
N7	3926.3(16)	5989.4(8)	7522.0(16)	16.4(3)
N3	2072.5(16)	6768.3(8)	5324.7(15)	14.8(3)
O00I	6182.6(19)	5352.9(10)	6497.1(17)	40.7(5)
N9	7107.9(16)	5463.6(8)	10275.3(16)	17.6(3)
N10	7557.6(17)	5394.9(8)	11646.8(17)	19.3(3)
C6	320.7(18)	6811.8(9)	3087.0(18)	13.3(3)
C3	957.2(19)	6538.1(9)	6791.5(18)	14.0(3)
C4	2085.6(19)	6386.7(9)	8077.8(18)	14.1(3)
C1	-487(2)	6589.0(10)	7796(2)	18.1(4)
C2	662(2)	6534.2(10)	9084(2)	18.7(4)
C8	5818.8(19)	5711.1(9)	9581.0(19)	14.9(3)
C7	3485.0(19)	6151.9(9)	8391.7(18)	14.5(3)

C5	979.1(18)	6649.1(9)	5477.5(18)	14.0(3)
C00T	5204(2)	7466.6(10)	2266(2)	19.1(4)
C00U	7879(2)	4954.7(10)	5563(2)	22.4(4)
C00V	6014(2)	6596.8(11)	4358(2)	27.1(5)
C00W	8472(3)	4733.9(12)	8209(2)	32.2(5)

Table S3: Anisotropic Displacement Parameters ($Å^2×10^3$) for **3**. The Anisotropic displacement factor exponent takes the form:$-2\pi^2$[h2a*2U11+2hka*b*U12+…].

Atom	**U11**	**U22**	**U33**	**U23**	**U13**	**U12**
S2	11.5(2)	18.9(2)	13.1(2)	-0.19(16)	7.36(17)	-0.40(16)
S002	14.6(2)	20.8(2)	18.5(2)	-2.20(18)	9.60(18)	-2.24(17)
S1	14.2(2)	17.9(2)	14.6(2)	-0.30(16)	6.69(17)	0.86(17)
S004	29.5(3)	25.8(3)	30.0(3)	6.1(2)	19.8(2)	5.8(2)
O005	13.5(6)	25.1(7)	17.8(7)	-1.2(5)	9.2(5)	-0.1(5)
O006	19.8(7)	32.5(8)	12.2(6)	4.2(6)	7.3(6)	3.5(6)
O007	19.5(7)	24.4(7)	28.8(7)	1.9(6)	18.4(6)	2.3(6)
O008	21.0(7)	28.3(8)	19.6(7)	3.7(6)	9.5(6)	0.7(6)
O009	17.3(7)	28.0(8)	27.1(8)	3.6(6)	2.6(6)	5.8(6)
N4	12.4(7)	21.6(8)	12.9(7)	1.7(6)	7.5(6)	0.7(6)
N2	18.1(8)	18.3(8)	14.0(7)	1.0(6)	8.3(6)	3.5(6)
N6	14.3(7)	15.7(7)	15.5(7)	1.7(6)	7.3(6)	1.2(6)
N8	15.5(8)	20.5(8)	16.9(8)	0.2(6)	8.2(7)	4.0(6)
N5	12.2(7)	19.6(8)	13.4(7)	1.0(6)	6.7(6)	1.7(6)
N1	16.1(8)	18.3(8)	16.1(8)	0.7(6)	8.8(6)	0.7(6)
N7	15.2(7)	17.8(8)	16.2(8)	0.2(6)	7.4(6)	3.3(6)
N3	13.5(7)	19.5(8)	13.0(7)	0.7(6)	7.5(6)	0.0(6)
O00I	49.4(11)	52.7(11)	32.6(9)	18.9(8)	29.8(8)	34.5(9)
N9	15.5(8)	17.8(8)	18.0(8)	0.6(6)	6.6(6)	2.3(6)
N10	15.9(8)	16.2(8)	21.9(8)	0.5(6)	5.6(7)	-1.5(6)
C6	13.6(8)	13.4(8)	15.6(8)	-0.3(6)	9.1(7)	1.3(6)
C3	15.5(8)	13.1(8)	15.6(8)	-1.9(6)	9.1(7)	-1.1(7)
C4	16.4(9)	12.7(8)	14.3(8)	-1.1(6)	8.2(7)	-0.4(7)
C1	16.3(9)	19.3(9)	21.4(9)	2.0(7)	11.2(8)	2.0(7)
C2	21.9(10)	21.1(10)	17.7(9)	1.6(7)	13.0(8)	2.9(7)
C8	14.5(8)	12.3(8)	18.1(9)	-0.9(7)	7.9(7)	-1.2(7)
C7	15.1(8)	13.4(8)	14.2(8)	0.9(7)	6.2(7)	-0.3(7)
C5	13.5(8)	14.7(8)	14.2(8)	-0.5(7)	6.7(7)	0.5(7)
C00T	15.7(9)	24.8(10)	19.9(9)	3.3(8)	10.9(8)	0.2(7)
C00U	26.2(10)	23.5(10)	21.6(10)	-0.6(8)	14.5(9)	1.5(8)
C00V	19.4(10)	29.7(11)	30.8(11)	12.4(9)	10.7(9)	7.1(9)
C00W	42.2(14)	35.3(13)	22.7(11)	10.0(9)	18.3(10)	18.6(10)

Table S4: Bond Lengths for **3.**

Atom	**Atom**	**Length/Å**	**Atom**	**Atom**	**Length/Å**
S2	C6	1.7284(18)	N2	C4	1.349(2)
S2	C5	1.7486(18)	N2	C2	1.327(2)
S002	O007	1.5221(14)	N6	N5	1.354(2)

S002	C00T	1.7827(19)	N8	N7	1.361(2)
S002	C00V	1.775(2)	N8	C8	1.339(2)
S1	C8	1.7302(19)	N5	C6	1.341(2)
S1	C7	1.7516(18)	N1	C3	1.344(2)
S004	O00I	1.5101(17)	N1	C1	1.339(2)
S004	C00U	1.780(2)	N7	C7	1.295(2)
S004	C00W	1.783(2)	N3	C5	1.296(2)
O005	N6	1.2479(19)	N9	N10	1.358(2)
O006	N6	1.233(2)	N9	C8	1.338(2)
O008	N10	1.248(2)	C3	C4	1.406(3)
O009	N10	1.236(2)	C3	C5	1.473(2)
N4	N3	1.361(2)	C4	C7	1.470(2)
N4	C6	1.342(2)	C1	C2	1.388(3)

Table S5: Bond Angles for **3**.

Atom	**Atom**	**Atom**	**Angle/°**	**Atom**	**Atom**	**Atom**	**Angle/°**
C6	S2	C5	87.46(9)	O009	N10	N9	115.97(16)
O007	S002	C00T	104.88(9)	N4	C6	S2	110.14(13)
O007	S002	C00V	105.32(10)	N5	C6	S2	132.08(14)
C00V	S002	C00T	98.12(10)	N5	C6	N4	117.75(16)
C8	S1	C7	87.71(9)	N1	C3	C4	120.35(16)
O00I	S004	C00U	105.10(10)	N1	C3	C5	111.74(16)
O00I	S004	C00W	105.51(11)	C4	C3	C5	127.91(16)
C00U	S004	C00W	98.96(11)	N2	C4	C3	119.81(16)
C6	N4	N3	117.08(15)	N2	C4	C7	111.37(16)
C2	N2	C4	118.58(16)	C3	C4	C7	128.72(16)
O005	N6	N5	121.33(15)	N1	C1	C2	120.69(17)
O006	N6	O005	122.52(15)	N2	C2	C1	121.22(17)
O006	N6	N5	116.14(15)	N8	C8	S1	109.84(13)
C8	N8	N7	117.42(15)	N9	C8	S1	131.78(15)
C6	N5	N6	114.39(15)	N9	C8	N8	118.38(16)
C1	N1	C3	118.32(16)	N7	C7	S1	115.38(14)
C7	N7	N8	109.62(15)	N7	C7	C4	127.22(17)
C5	N3	N4	109.45(15)	C4	C7	S1	117.11(13)
C8	N9	N10	114.19(16)	N3	C5	S2	115.77(14)
O008	N10	N9	121.59(16)	N3	C5	C3	126.13(17)
O009	N10	O008	122.44(17)	C3	C5	S2	118.00(13)

Table S6: Torsion Angles for **6.**

A	**B**	**C**	**D**	**Angle/°**	**A**	**B**	**C**	**D**	**Angle/°**
O005	N6	N5	C6	3.9(2)	C6	N4	N3	C5	0.5(2)
O006	N6	N5	C6	-176.75(16)	C3	N1	C1	C2	2.6(3)
N4	N3	C5	S2	-2.6(2)	C3	C4	C7	S1	-179.21(15)
N4	N3	C5	C3	-178.81(17)	C3	C4	C7	N7	-5.6(3)
N2	C4	C7	S1	-3.0(2)	C4	N2	C2	C1	4.2(3)
N2	C4	C7	N7	170.59(18)	C4	C3	C5	S2	167.93(15)

N6	N5	C6	S2	8.7(3)	C4	C3	C5	N3	-15.9(3)
N6	N5	C6	N4	-173.29(15)	C1	N1	C3	C4	6.7(3)
N8	N7	C7	S1	-1.8(2)	C1	N1	C3	C5	-172.80(16)
N8	N7	C7	C4	-175.55(17)	C2	N2	C4	C3	5.0(3)
N1	C3	C4	N2	-10.7(3)	C2	N2	C4	C7	-171.56(16)
N1	C3	C4	C7	165.16(18)	C8	S1	C7	N7	1.30(15)
N1	C3	C5	S2	-12.6(2)	C8	S1	C7	C4	175.68(15)
N1	C3	C5	N3	163.49(18)	C8	N8	N7	C7	1.6(2)
N1	C1	C2	N2	-8.4(3)	C8	N9	N10	O008	0.6(2)
N7	N8	C8	S1	-0.6(2)	C8	N9	N10	O009	179.83(16)
N7	N8	C8	N9	178.53(16)	C7	S1	C8	N8	-0.34(14)
N3	N4	C6	S2	1.8(2)	C7	S1	C8	N9	-179.34(19)
N3	N4	C6	N5	-176.64(16)	C5	S2	C6	N4	-2.55(14)
N10	N9	C8	S1	3.7(3)	C5	S2	C6	N5	175.60(19)
N10	N9	C8	N8	-175.19(16)	C5	C3	C4	N2	168.64(17)
C6	S2	C5	N3	3.07(15)	C5	C3	C4	C7	-15.5(3)
C6		S2		C5		C3		179.60(15)	

Table S7: Hydrogen Atom Coordinates (Å×104) and Isotropic Displacement Parameters (Å^2×10^3) for **3.**

Atom	***x***	***y***	***z***	**U(eq)**
H4	2301.95	6939.27	3679.19	18
H8	5712.95	5626.99	7771.18	21
H1	-1393.44	6616.17	7721.35	22
H2	545.03	6584.24	9882.68	22
H00A	4460.21	7704.24	1493.62	29
H00B	5801.41	7238.88	1950.41	29
H00C	5760.04	7785.71	2990.46	29
H00G	7199.75	4980.82	4586.79	34
H00H	8576.67	4613.75	5693.83	34
H00I	8338.84	5387.7	5871.19	34
H00D	6508.4	6982.33	4922.26	41
H00E	6607.49	6372.99	4032.36	41
H00F	5785.92	6285.07	4910.02	41
H00J	8966.35	5160.06	8376.22	48
H00K	9101.04	4370.03	8271.08	48
H00L	8152.1	4668.13	8899.83	48

NMR, IR Spectra, HRMS & TG-DSC plots for 2-7.

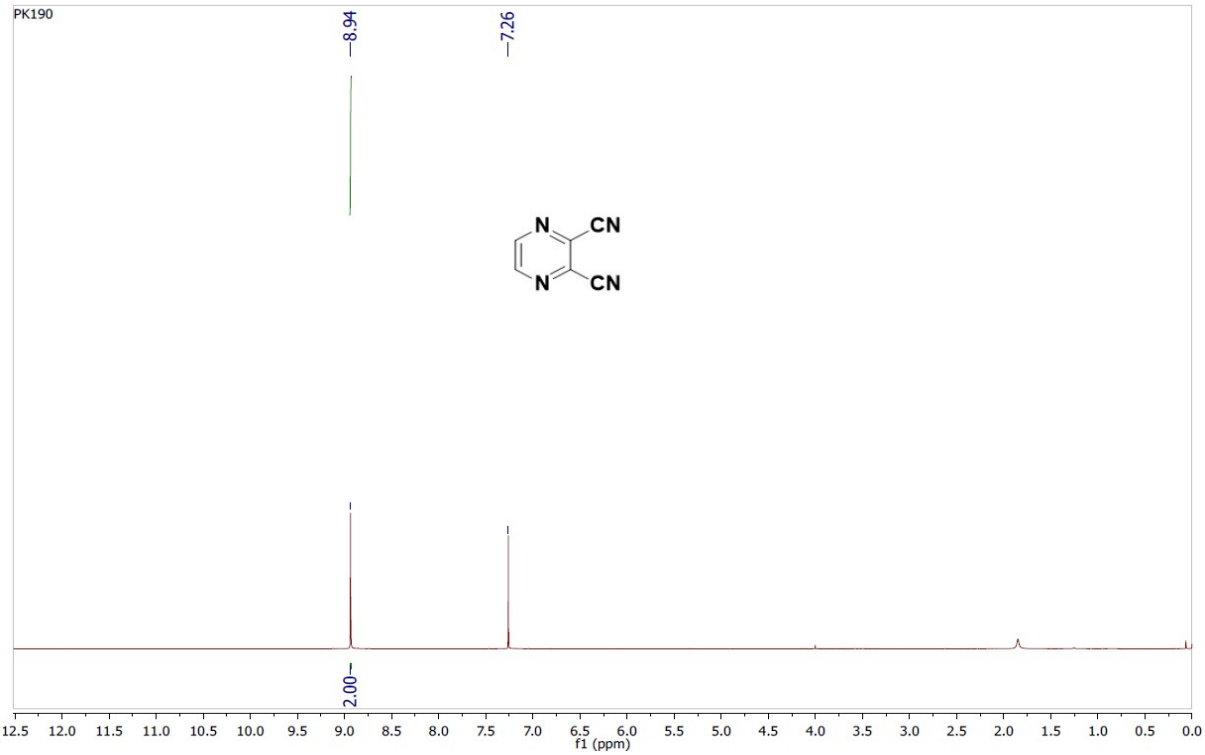

Figure S2: ^{1}H NMR spectrum of compound **1** in **$CDCl_3$**.

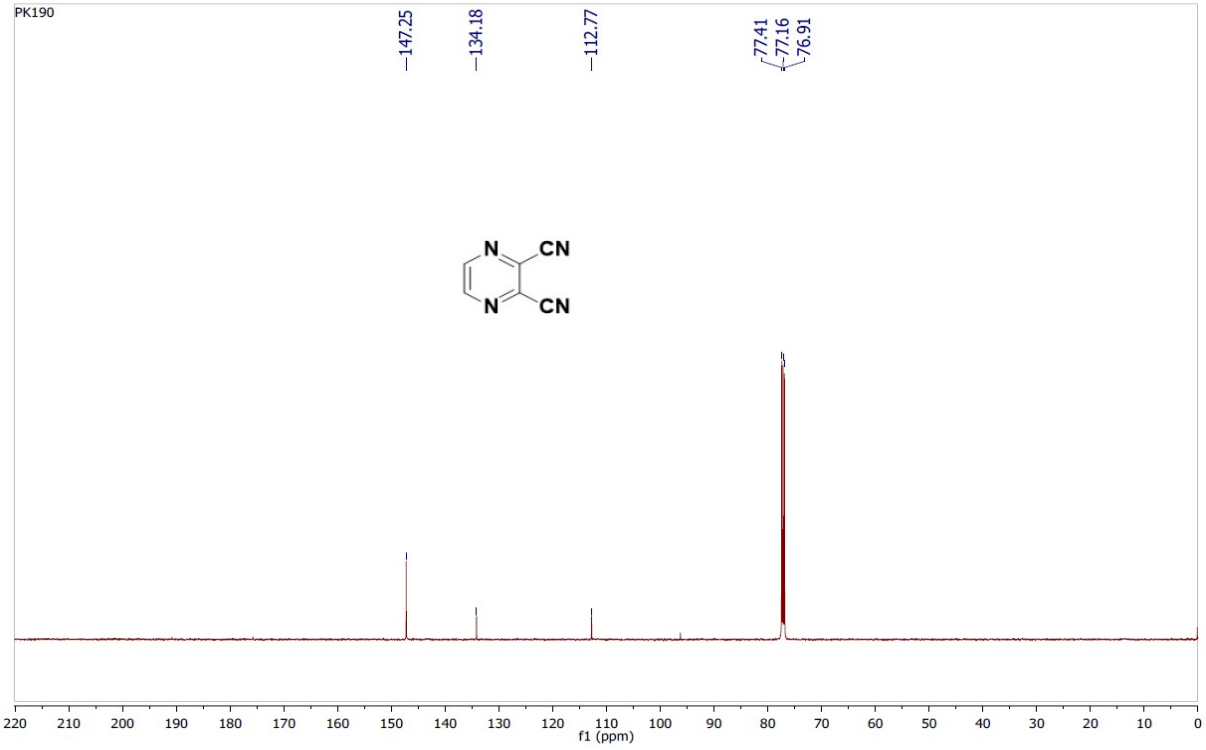

Figure S3: ^{13}C NMR spectrum of compound **1** in **$CDCl_3$.**

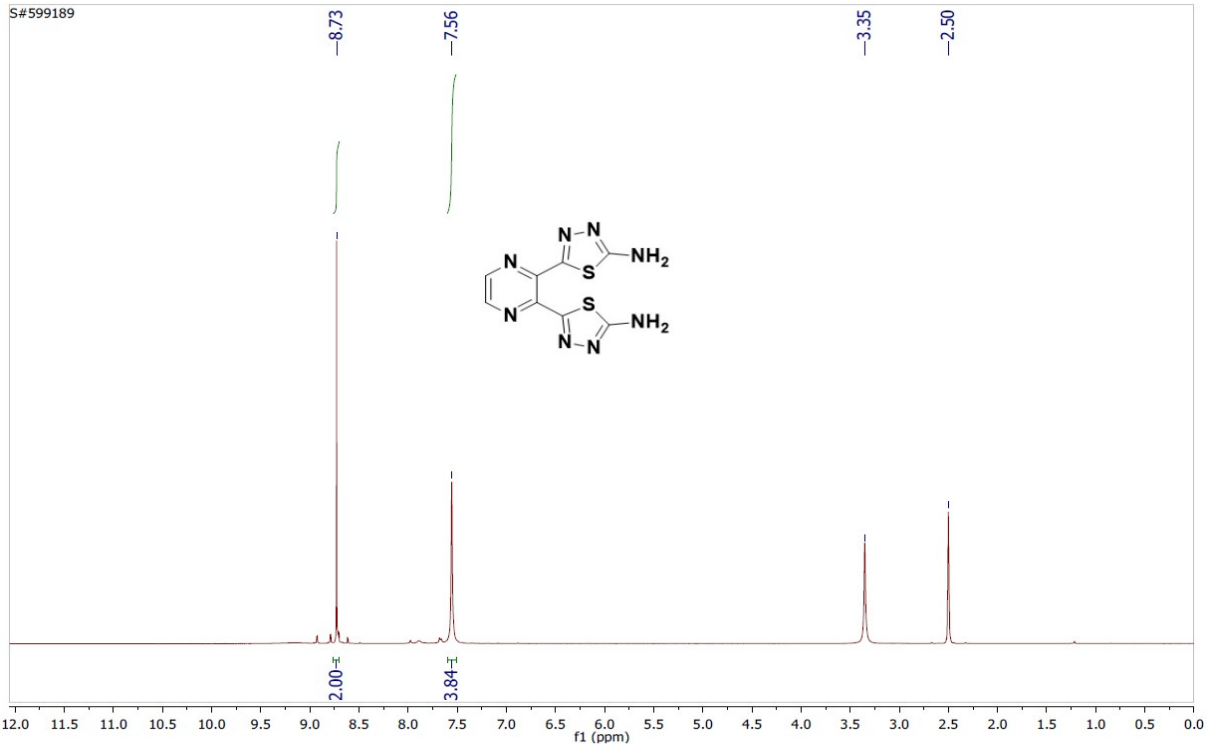

Figure S4: ^{1}H NMR spectrum of compound **2** in **DMSO-*d*$_6$**.

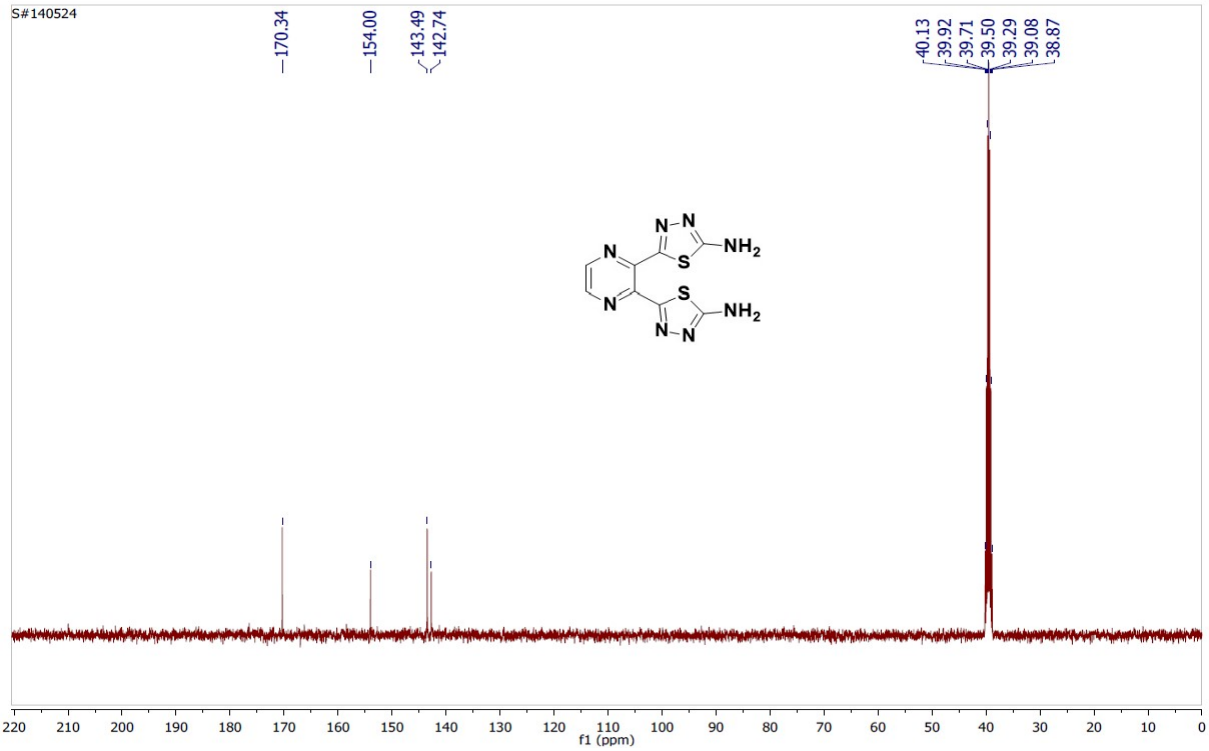

Figure S5: ^{13}C NMR spectrum of compound **2** in **DMSO-*d*$_6$.**

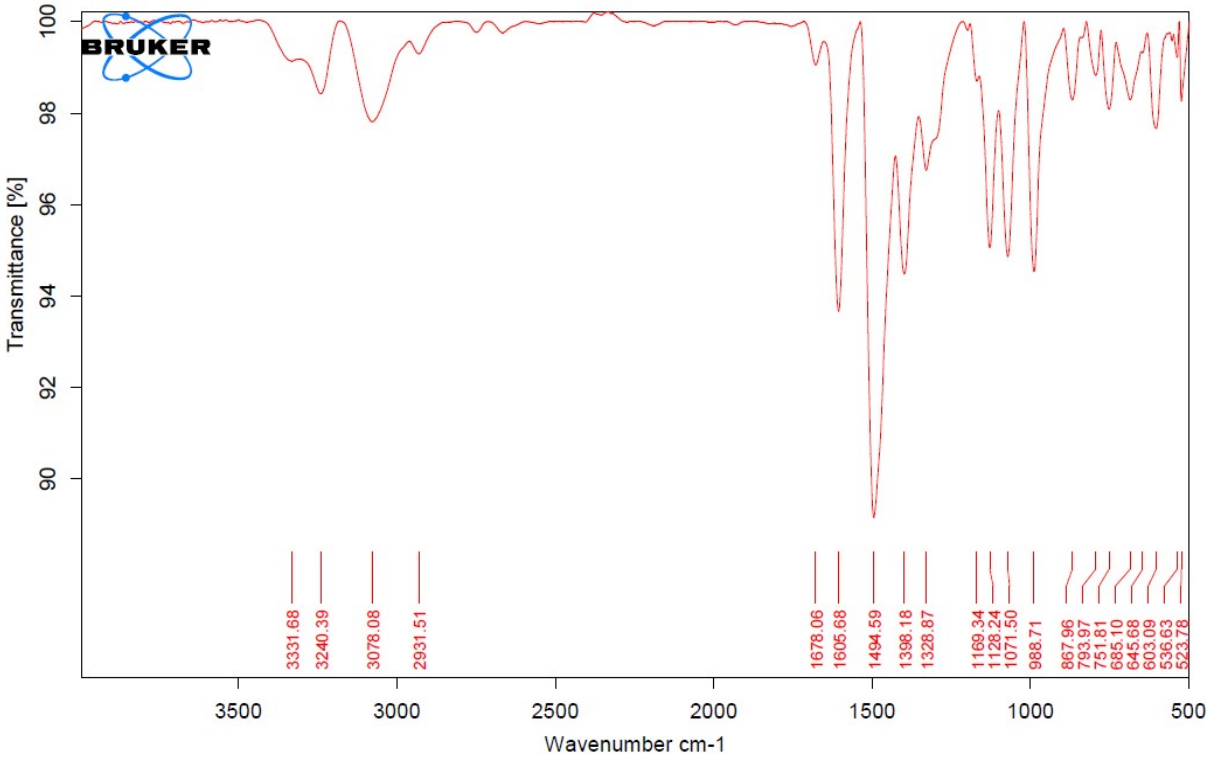

Figure S6: IR spectrum of compound **2.**

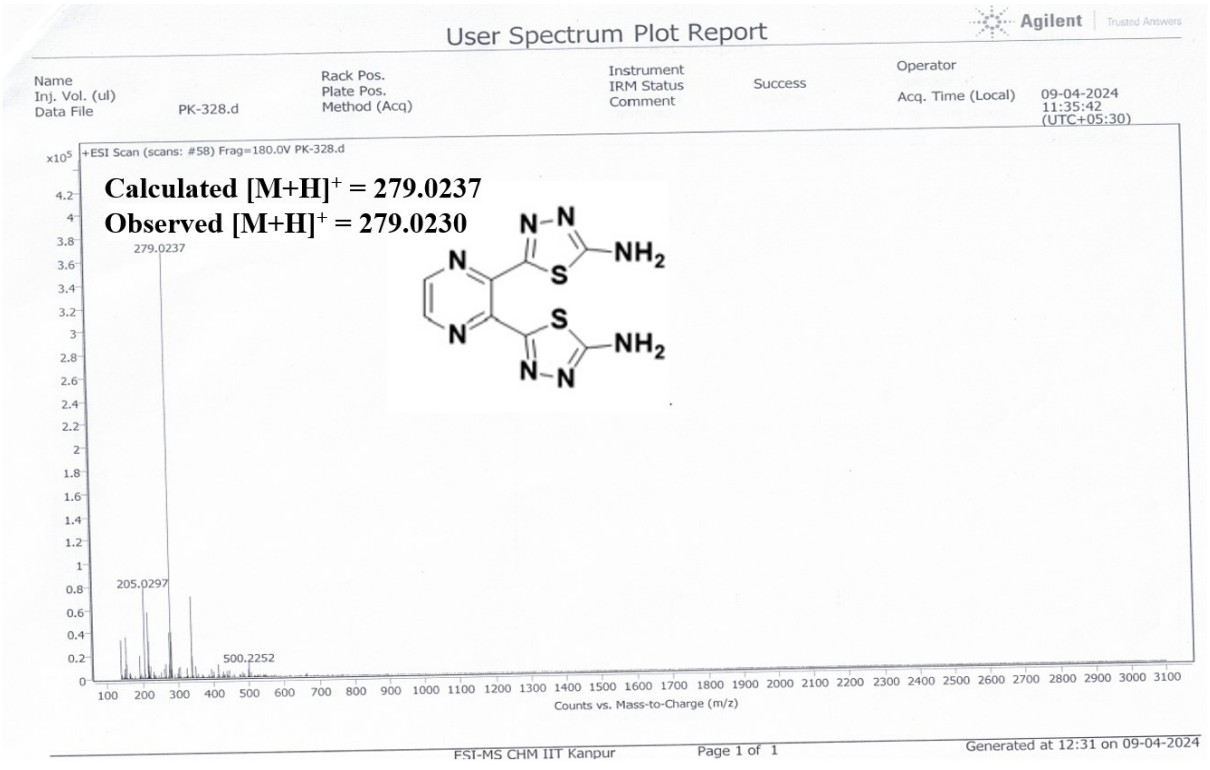

Figure S7: Mass spectrum of compound **2.**

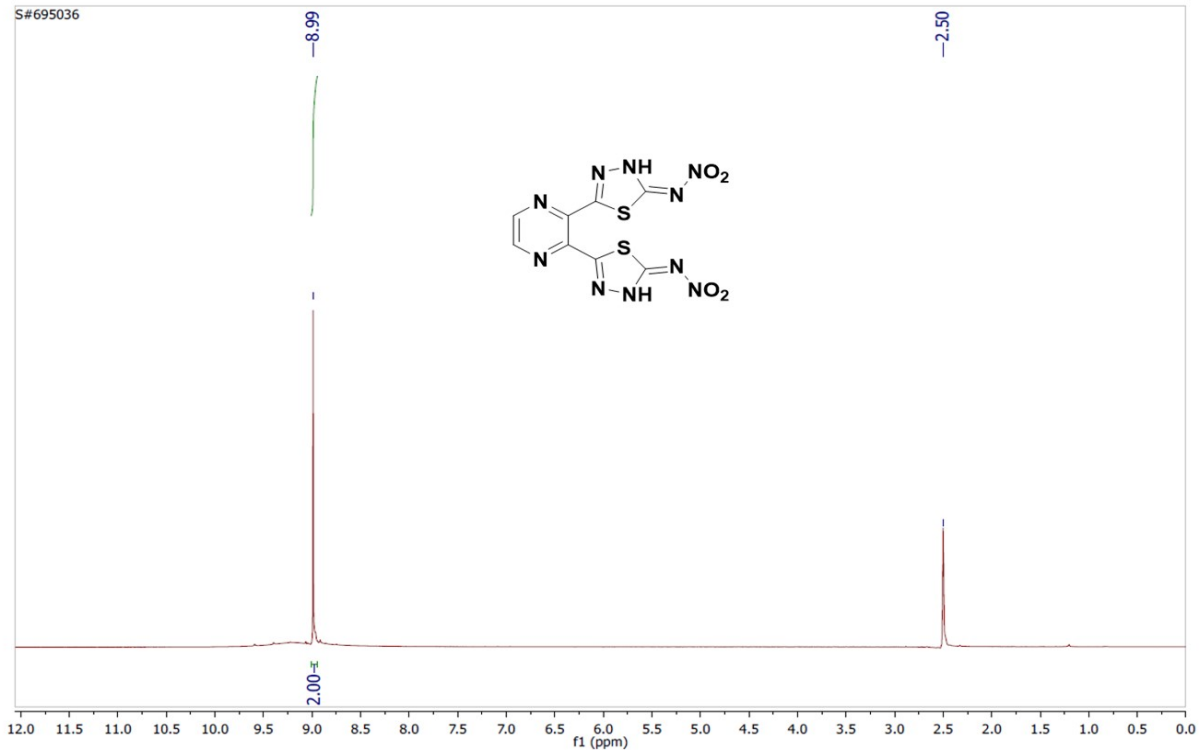

Figure S8: ^{1}H NMR spectrum of compound **3** in **DMSO-*d*$_6$.**

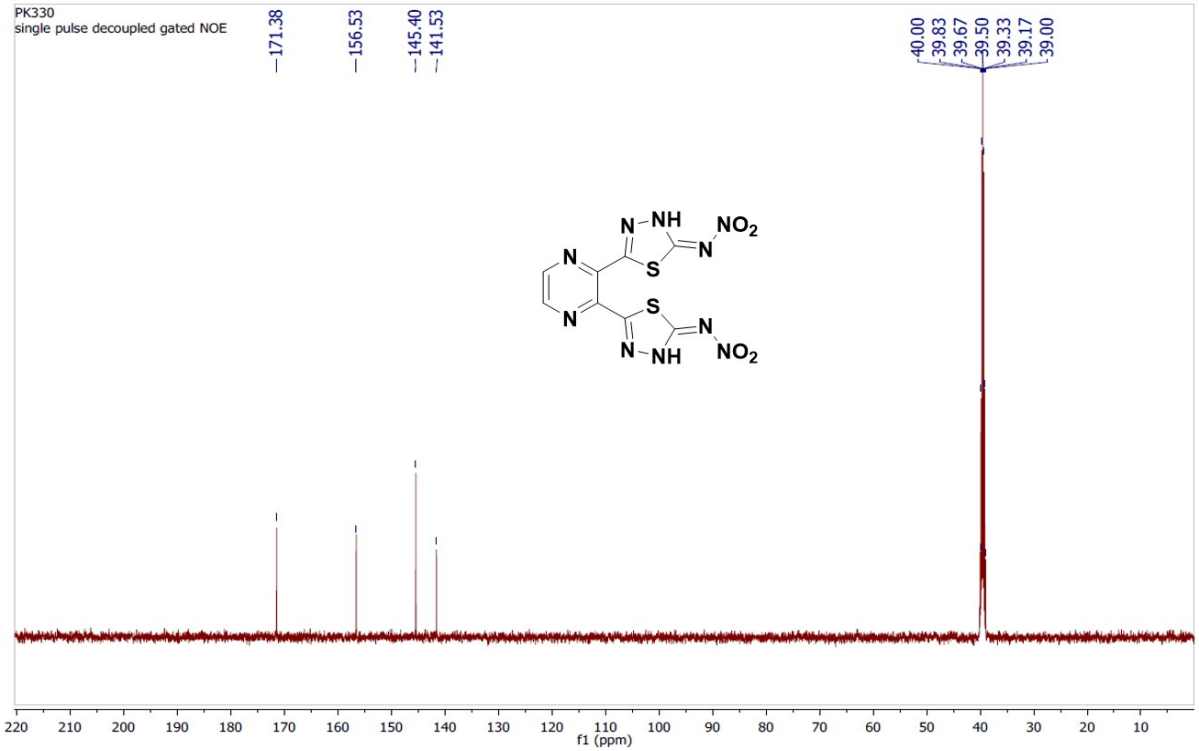

Figure S9: ^{13}C NMR spectrum of compound **3** in **DMSO-*d*$_6$.**

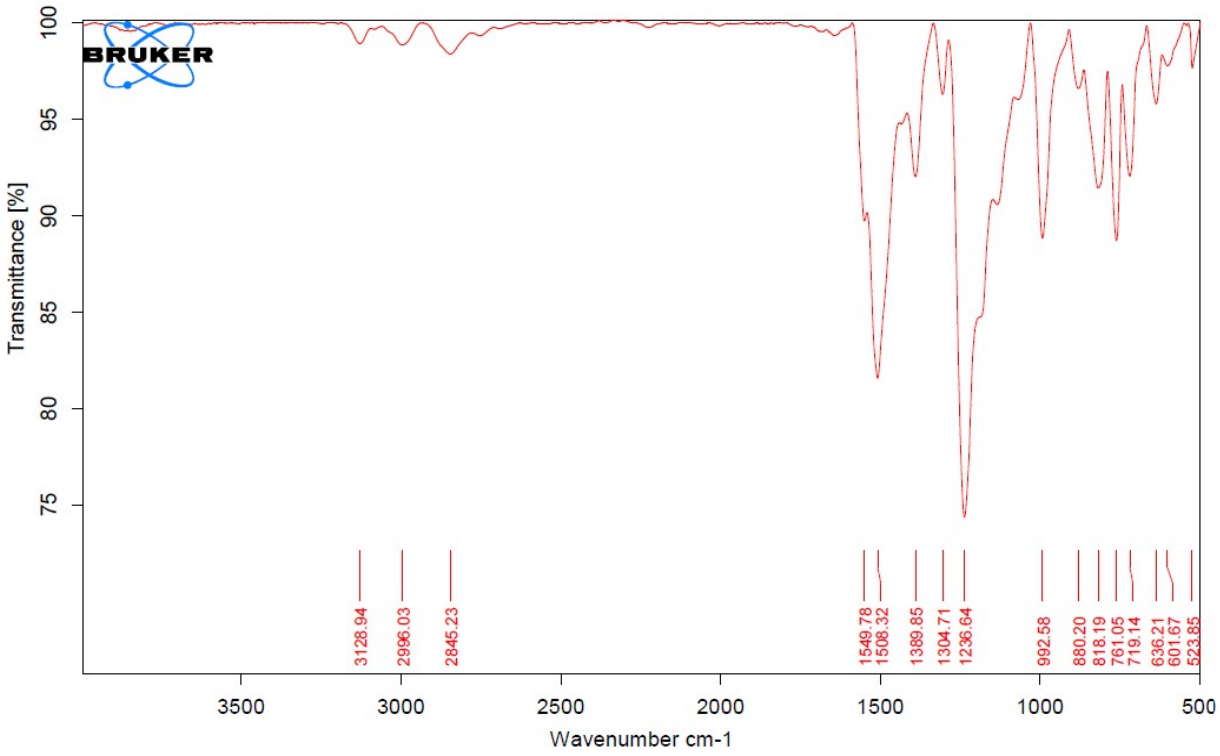

Figure S10: IR spectrum of compound **3.**

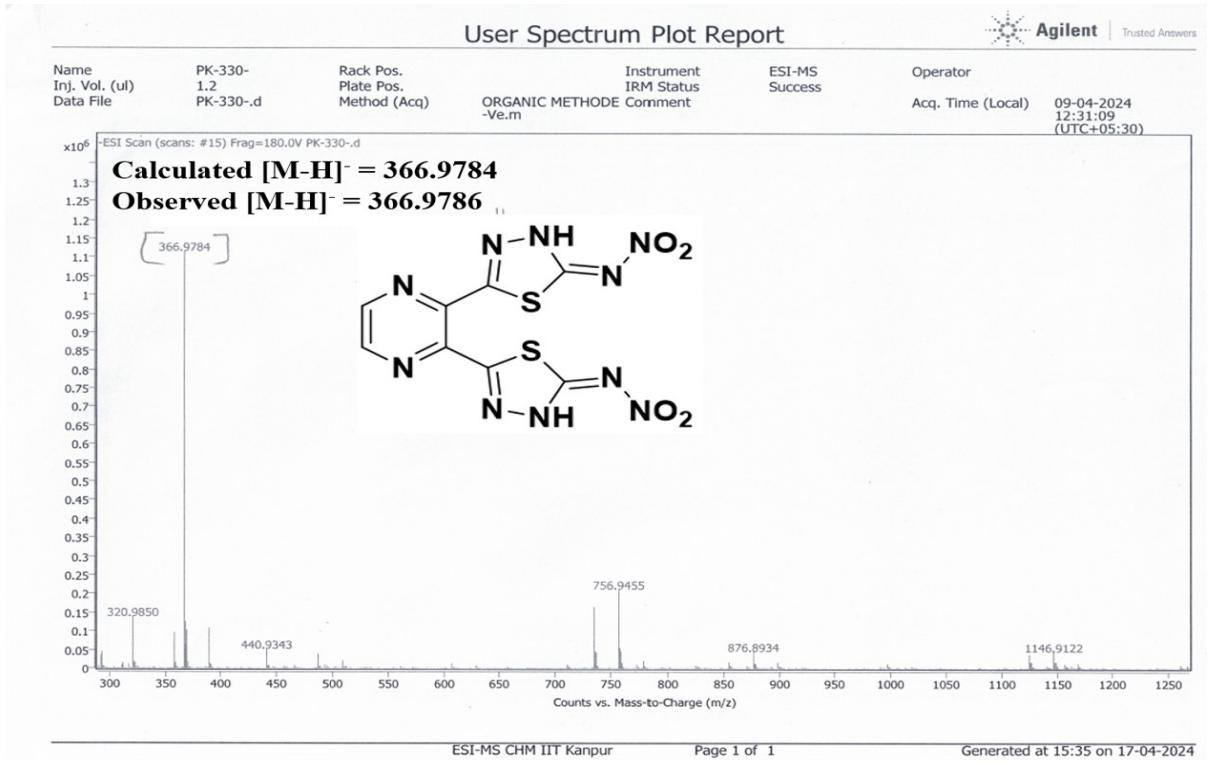

Figure S11: Mass spectrum of compound **3.**

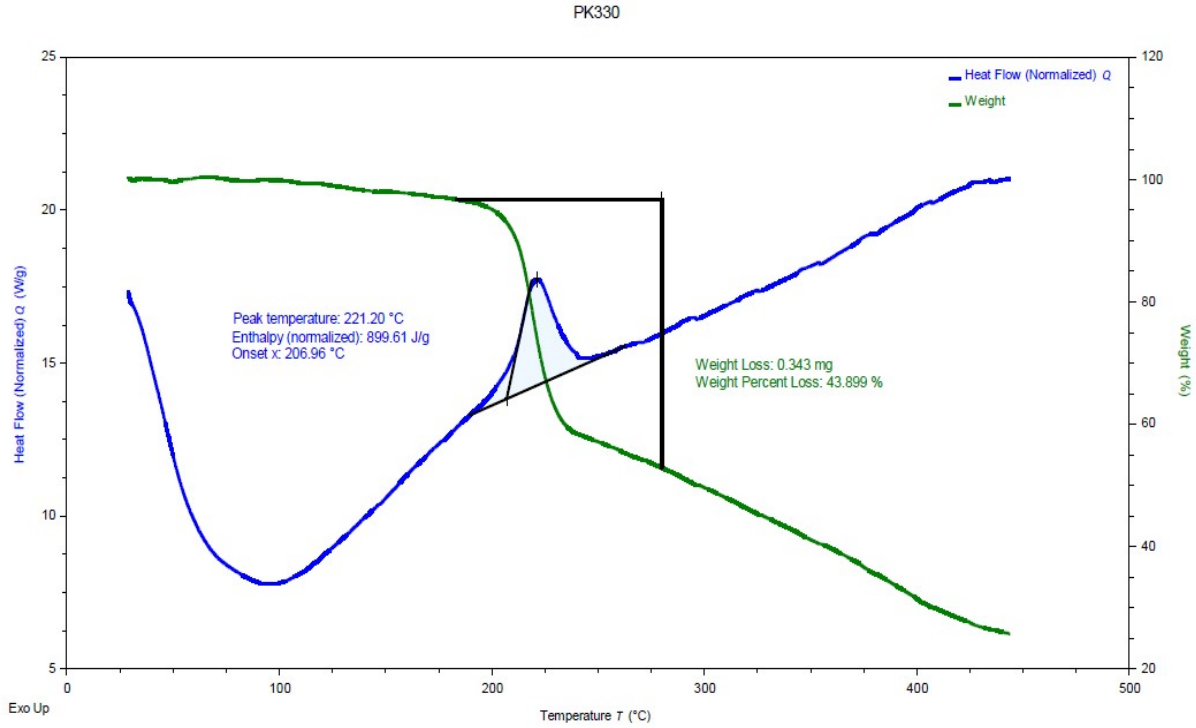

Figure S12: DSC spectrum of compound **3** at heating rate 5 °C min^{-1}**.**

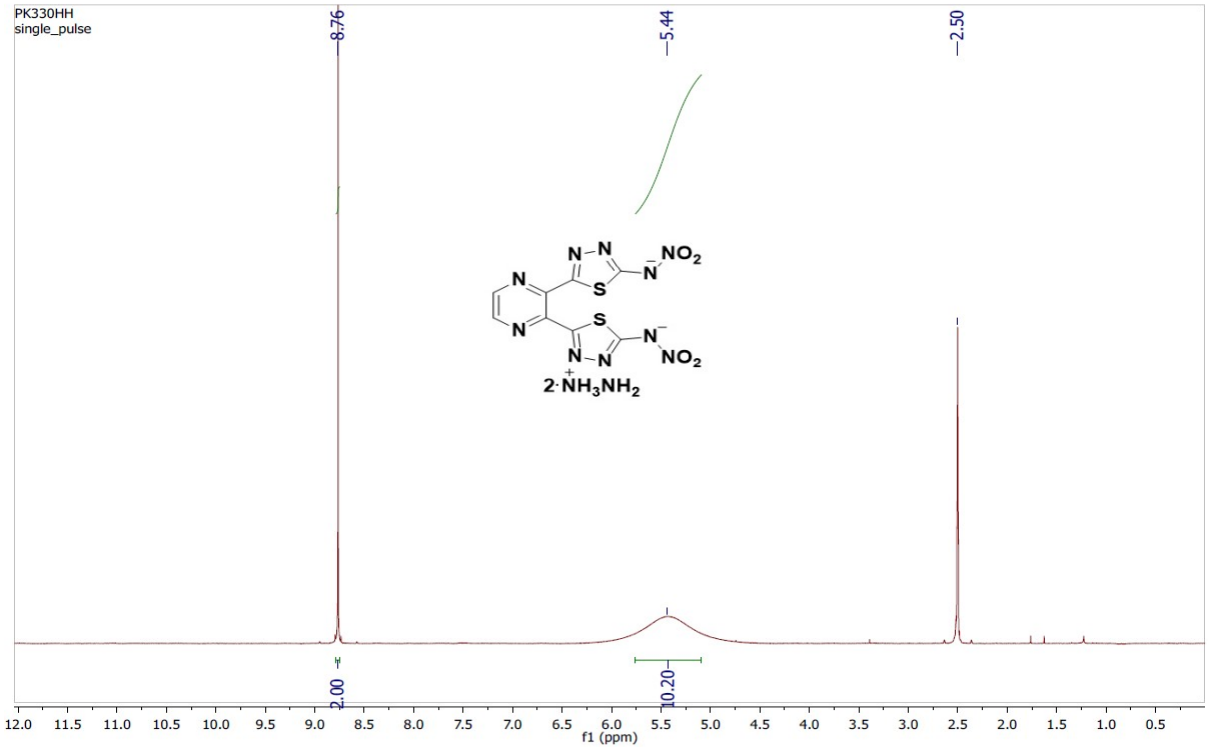

Figure S13: ^{1}H NMR spectrum of compound **4** in **DMSO-*d*$_6$**.

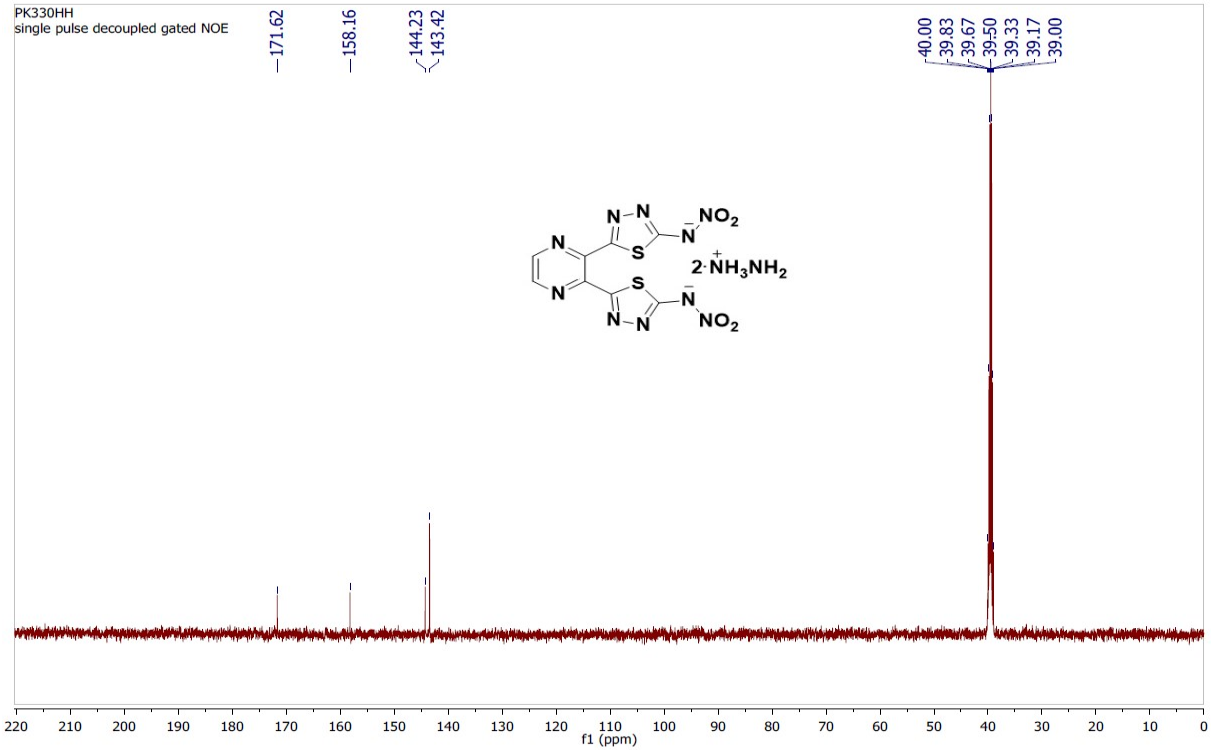

Figure S14: ^{13}C NMR spectrum of compound **4** in **DMSO-*d*$_6$.**

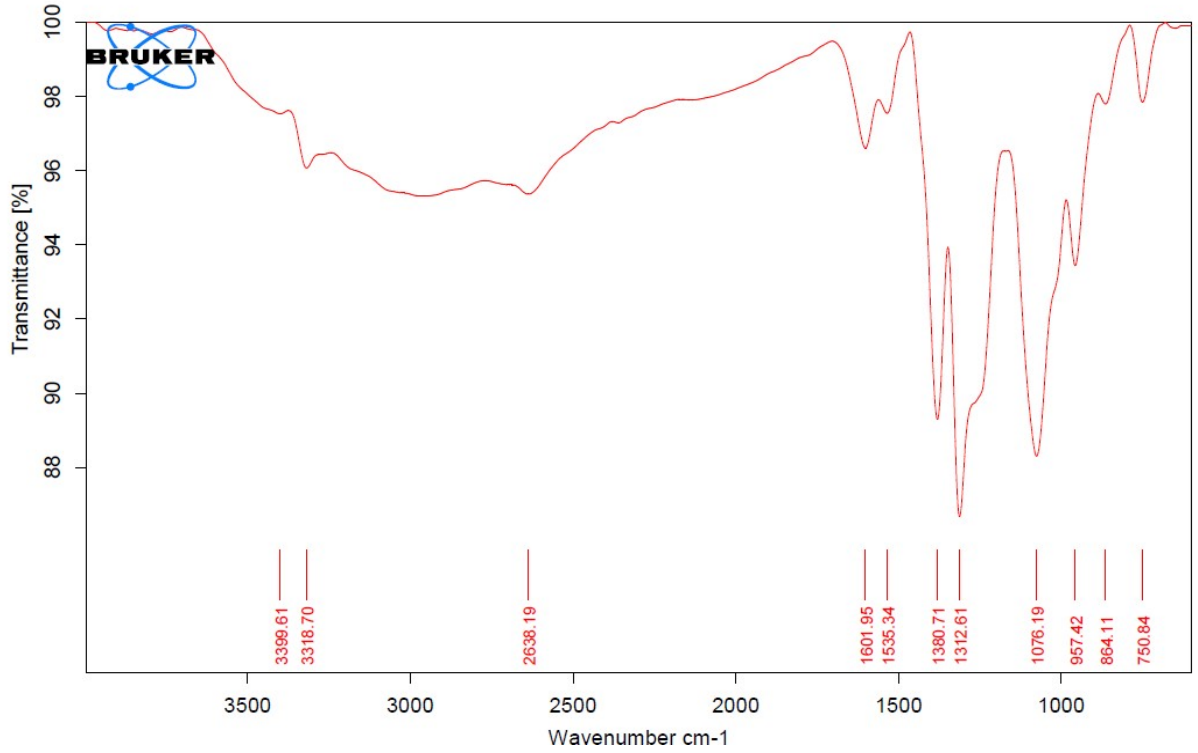

Figure S15: IR spectrum of compound **4.**

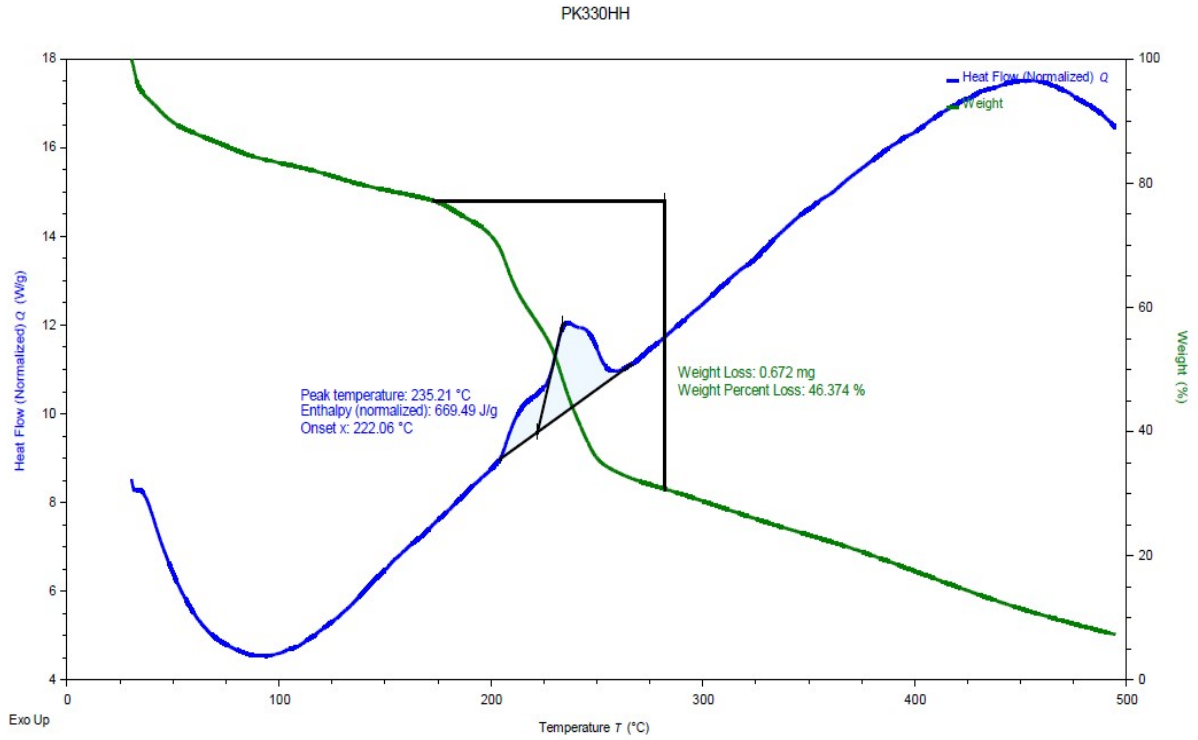

Figure S16: DSC spectrum of compound **4** at heating rate 5 °C min^{-1}**.**

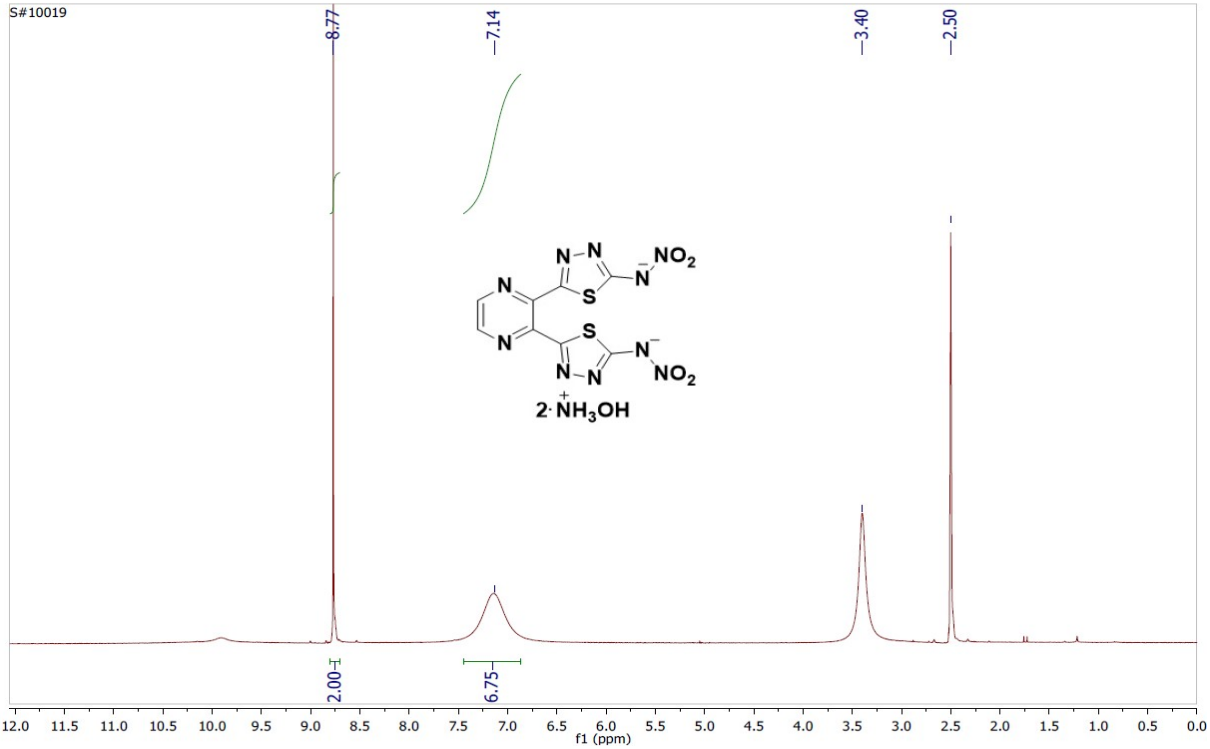

Figure S17: ^{1}H NMR spectrum of compound **5** in **DMSO-*d*$_6$.**

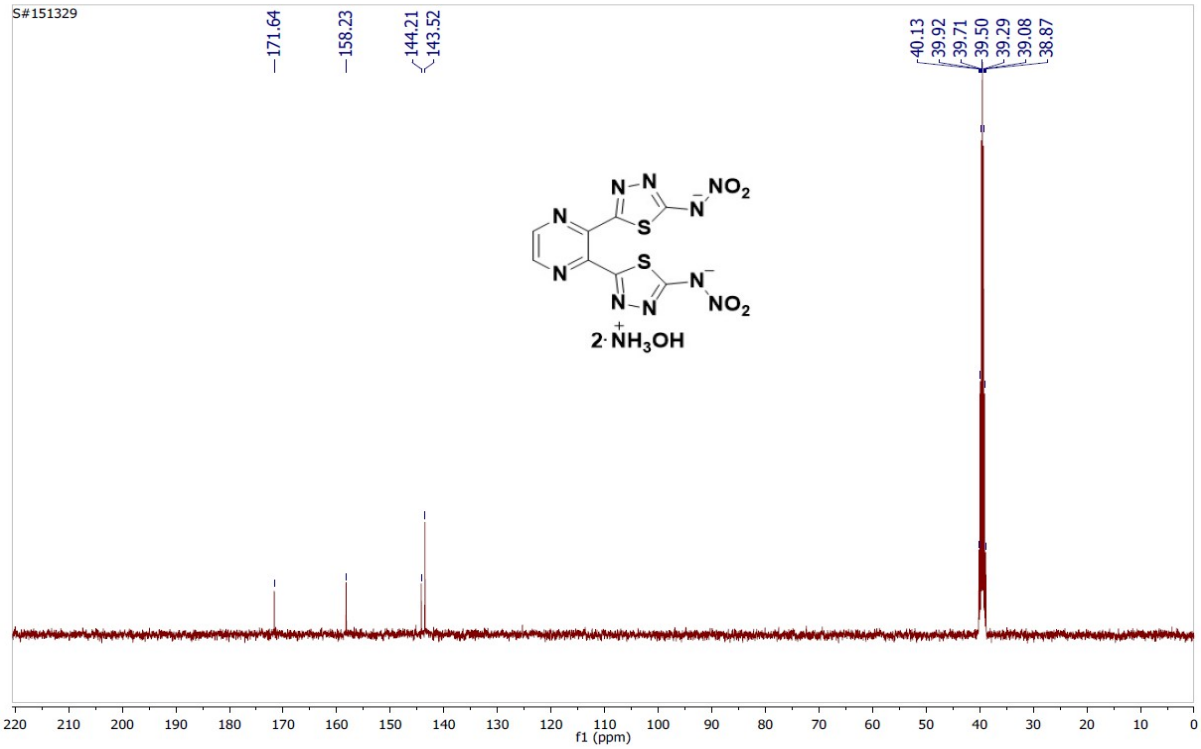

Figure S18: ^{13}C NMR spectrum of compound **5** in **DMSO-*d*$_6$.**

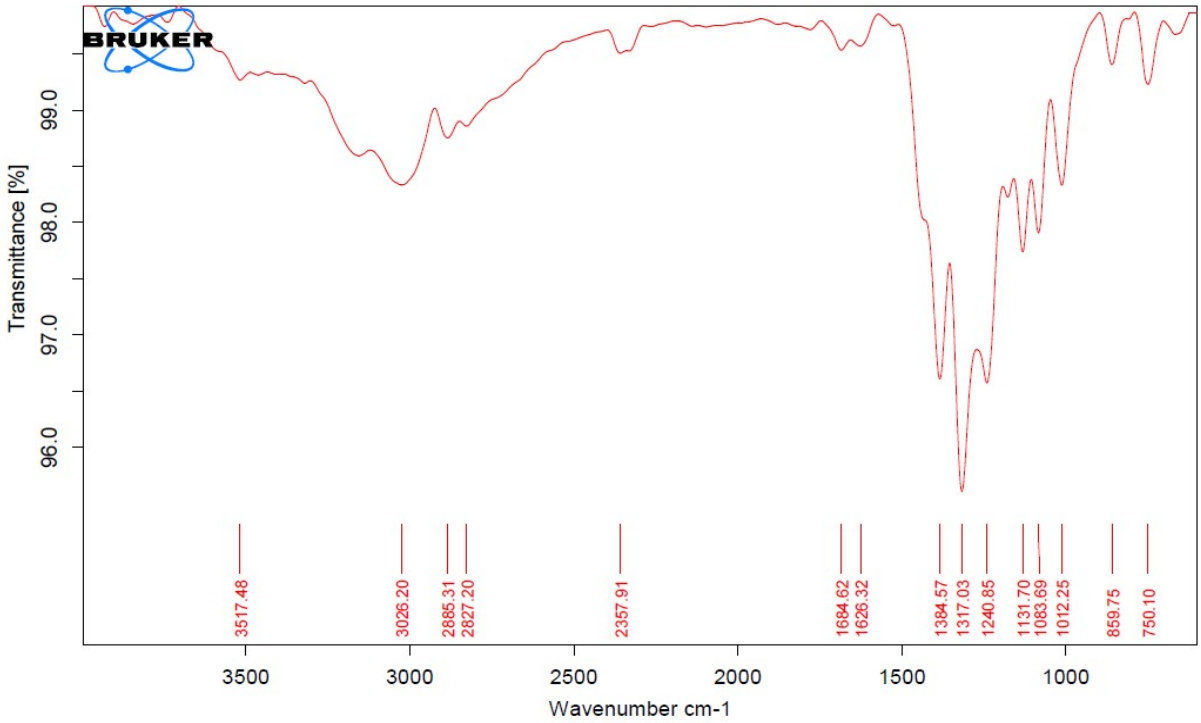

Figure S19: IR spectrum of compound **5.**

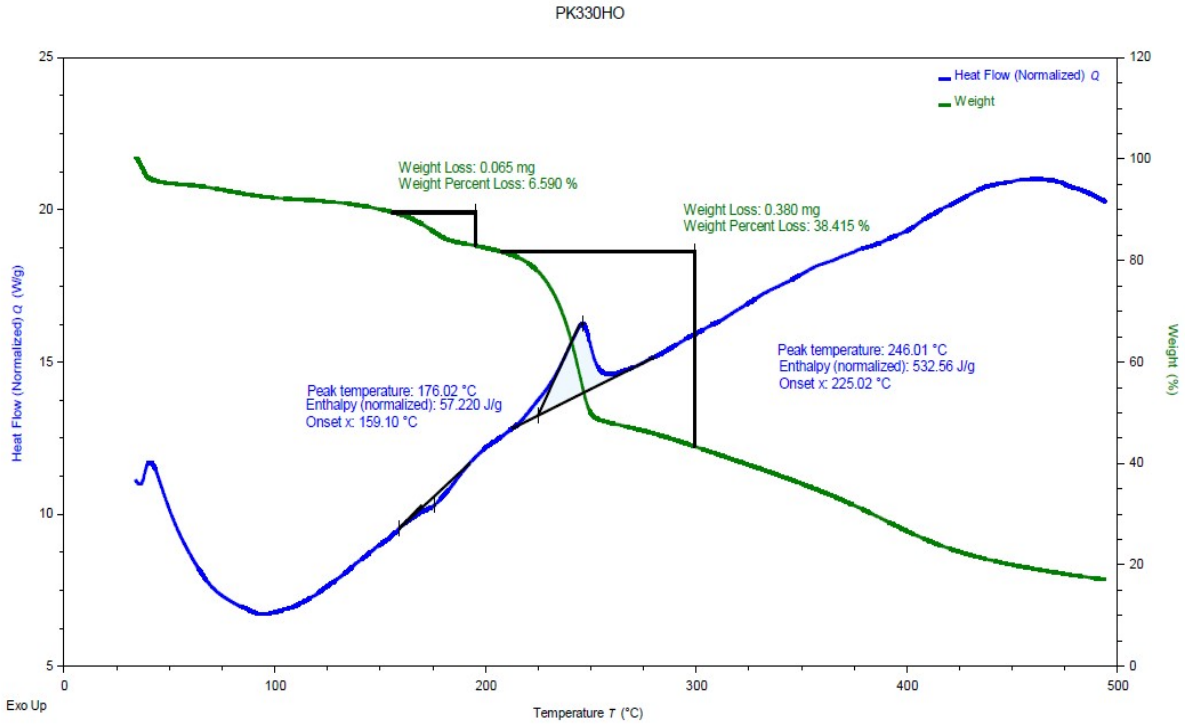

Figure S20: DSC spectrum of compound **5** at heating rate 5 °C min^{-1}**.**

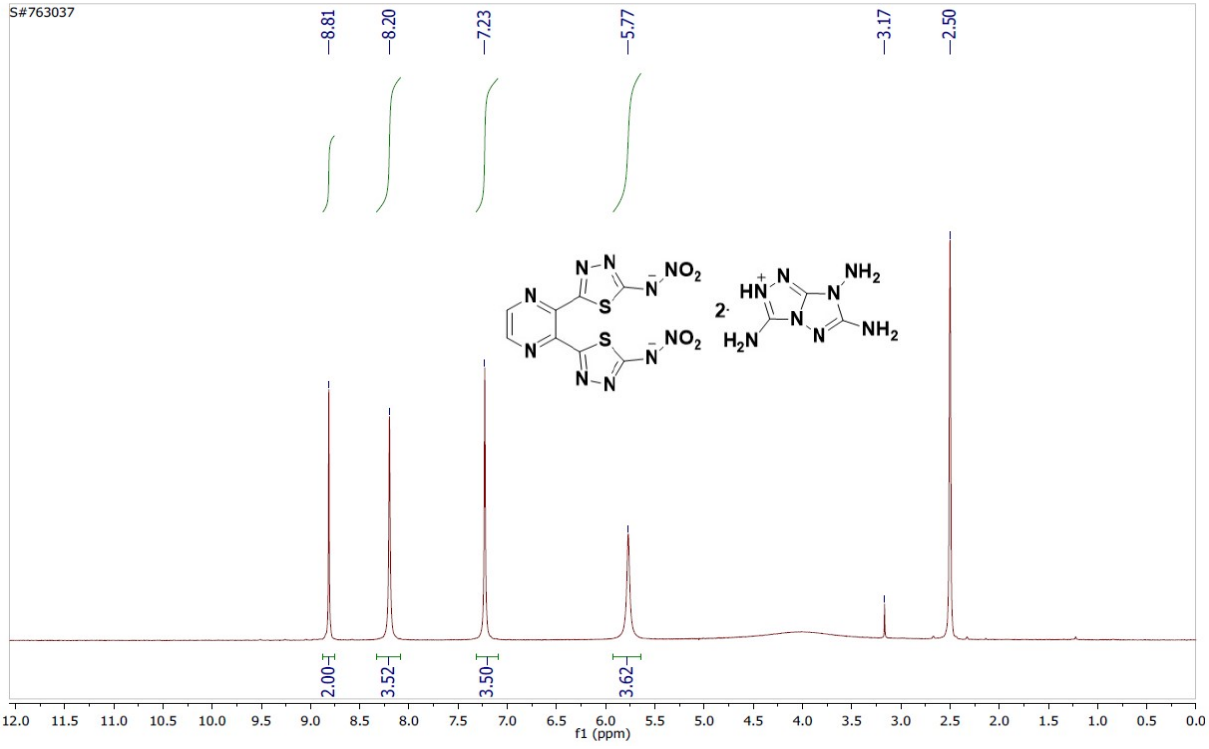

Figure S21: ^{1}H NMR spectrum of compound **6** in **DMSO-*d*$_6$**.

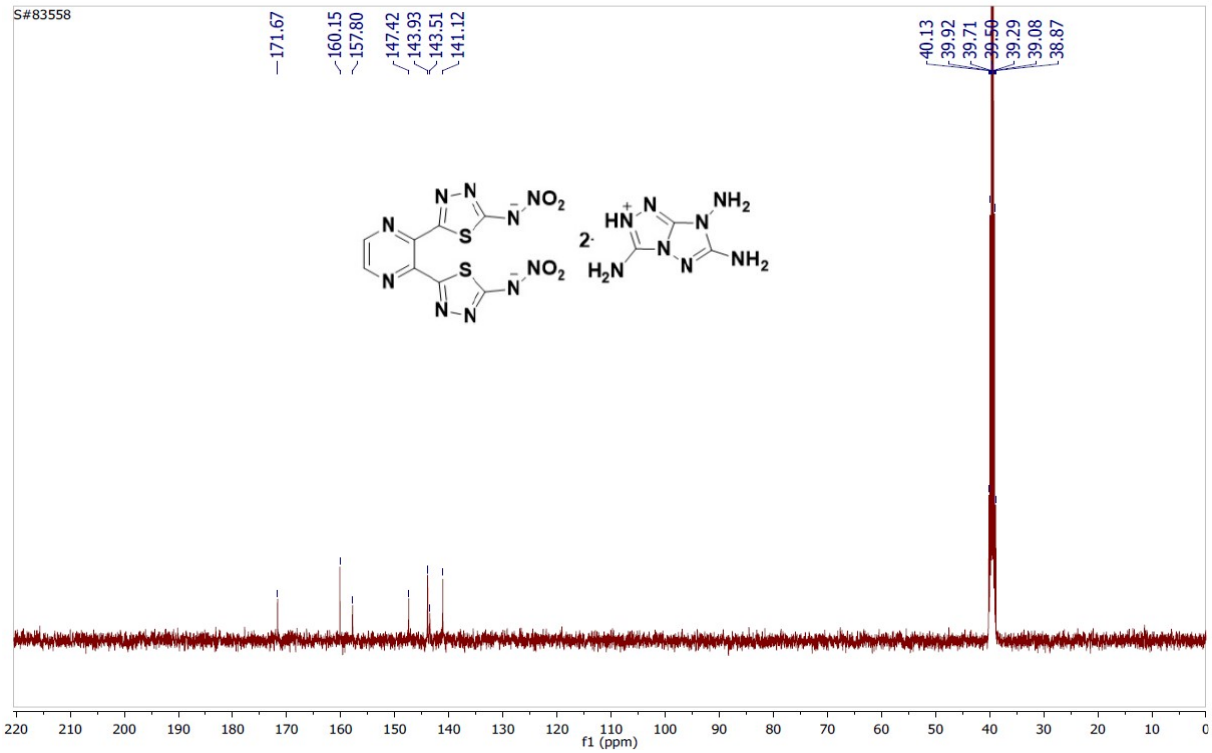

Figure S22: ^{13}C NMR spectrum of compound **6** in **DMSO-*d*$_6$.**

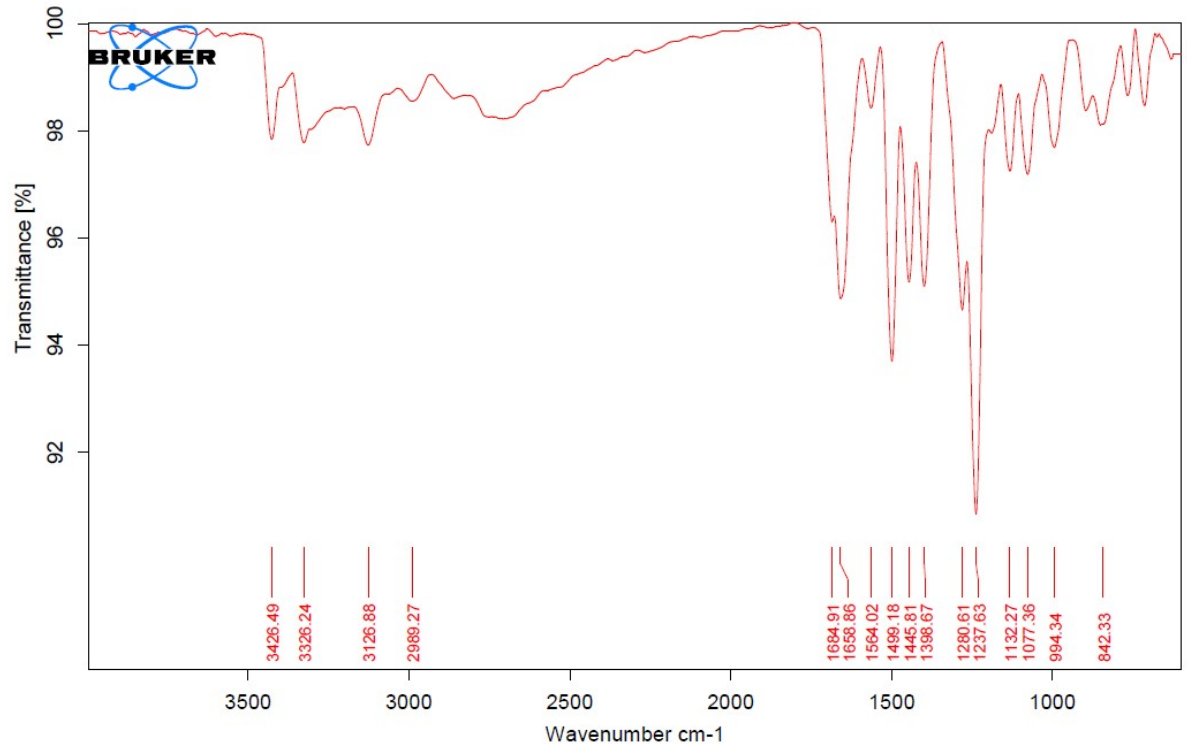

Figure S23: IR spectrum of compound **6.**

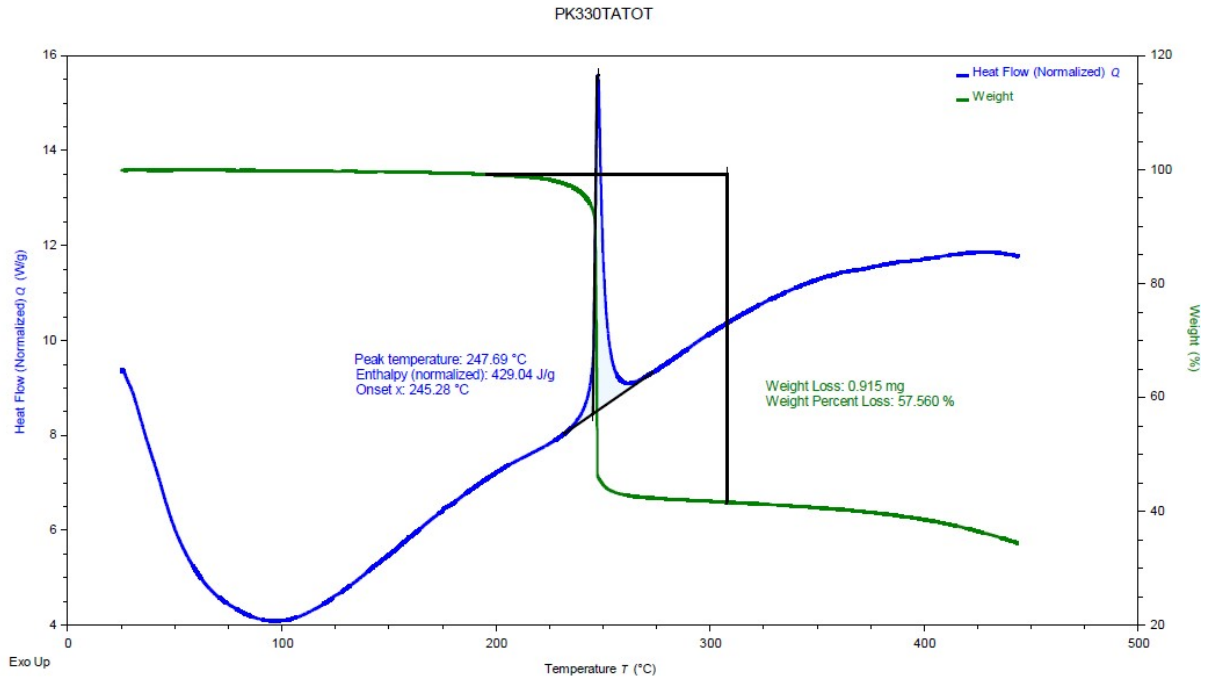

Figure S24. DSC spectrum of compound **6.**

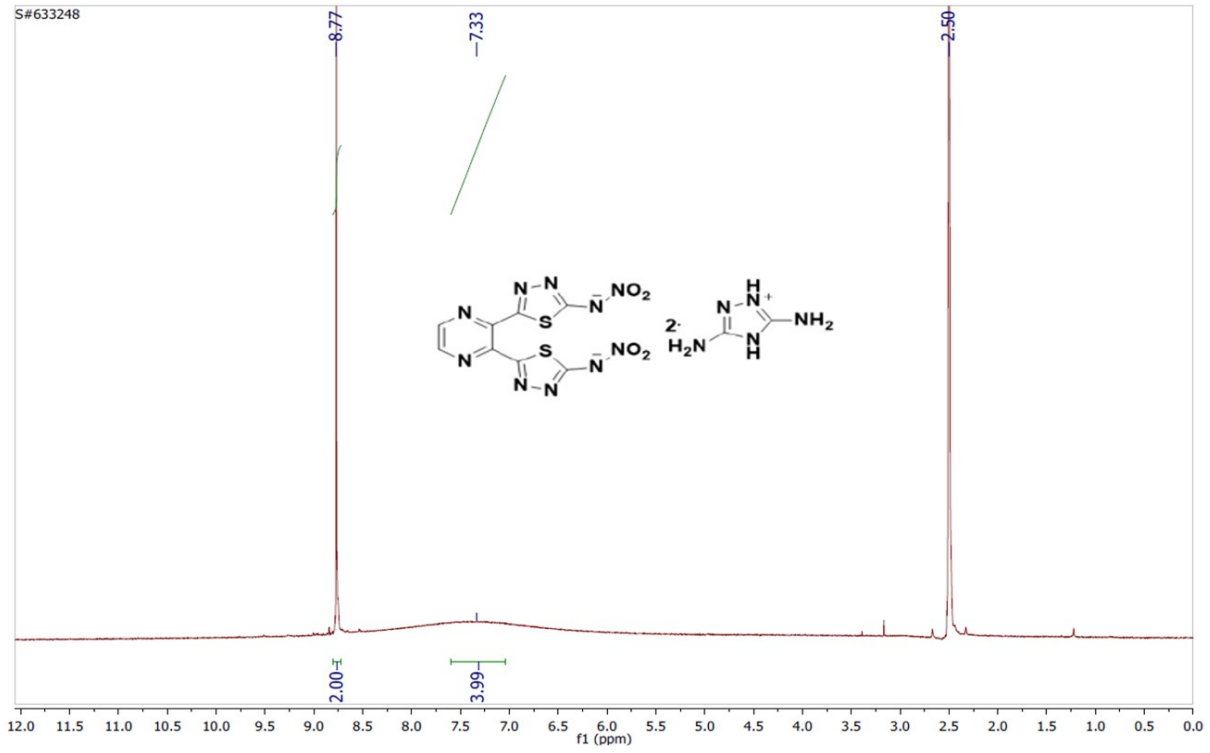

Figure S25: ^{1}H NMR spectrum of compound **7** in **DMSO-*d*$_6$**.

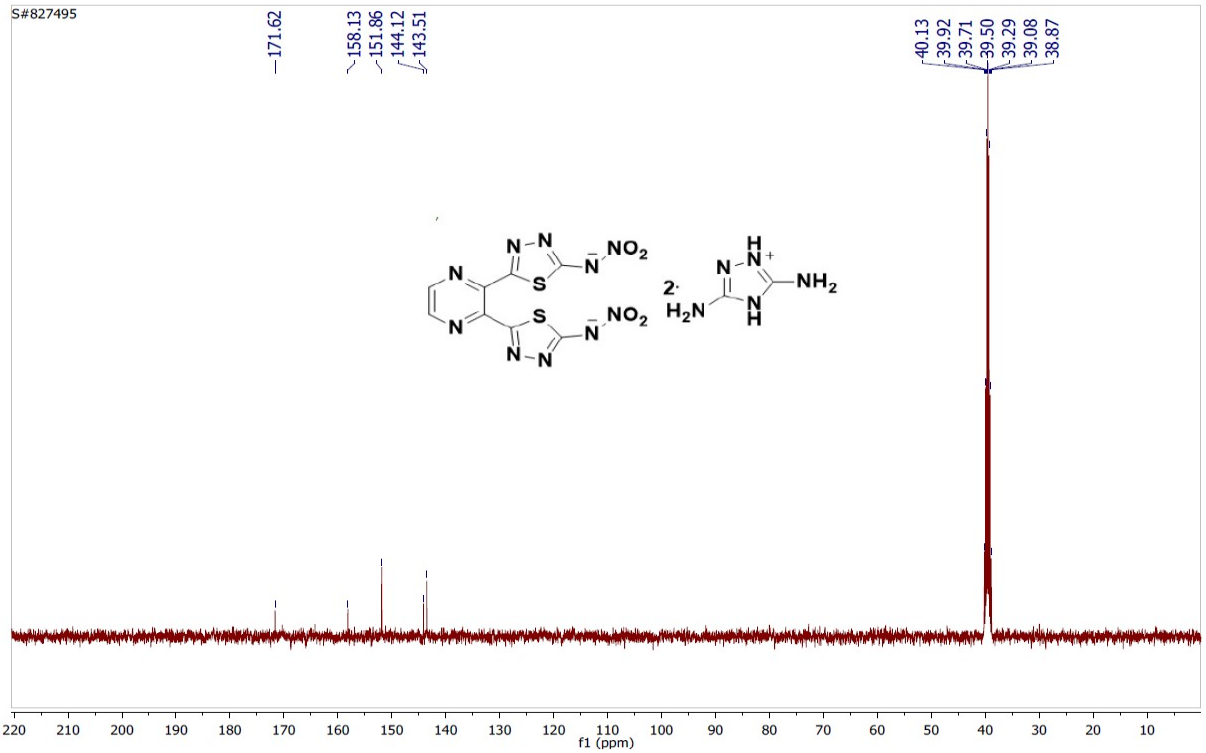

Figure S26: ^{13}C NMR spectrum of compound **7** in **DMSO-*d*$_6$.**

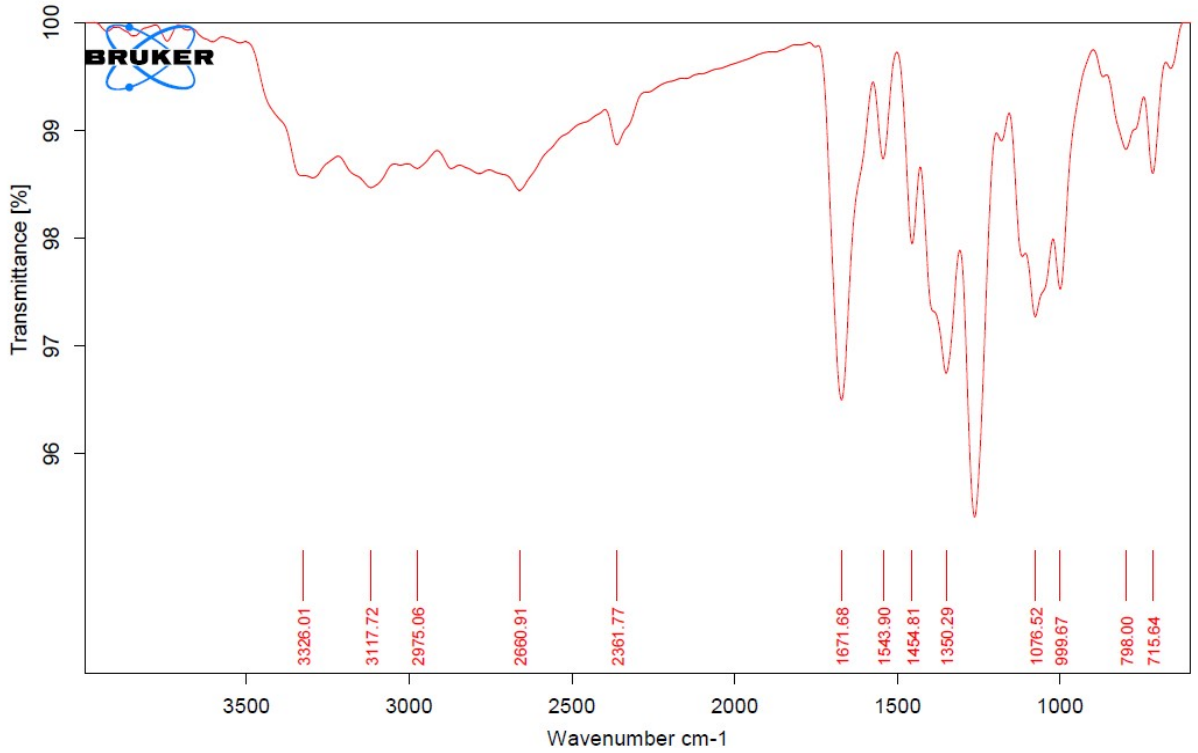

Figure S27: IR spectrum of compound **7.**

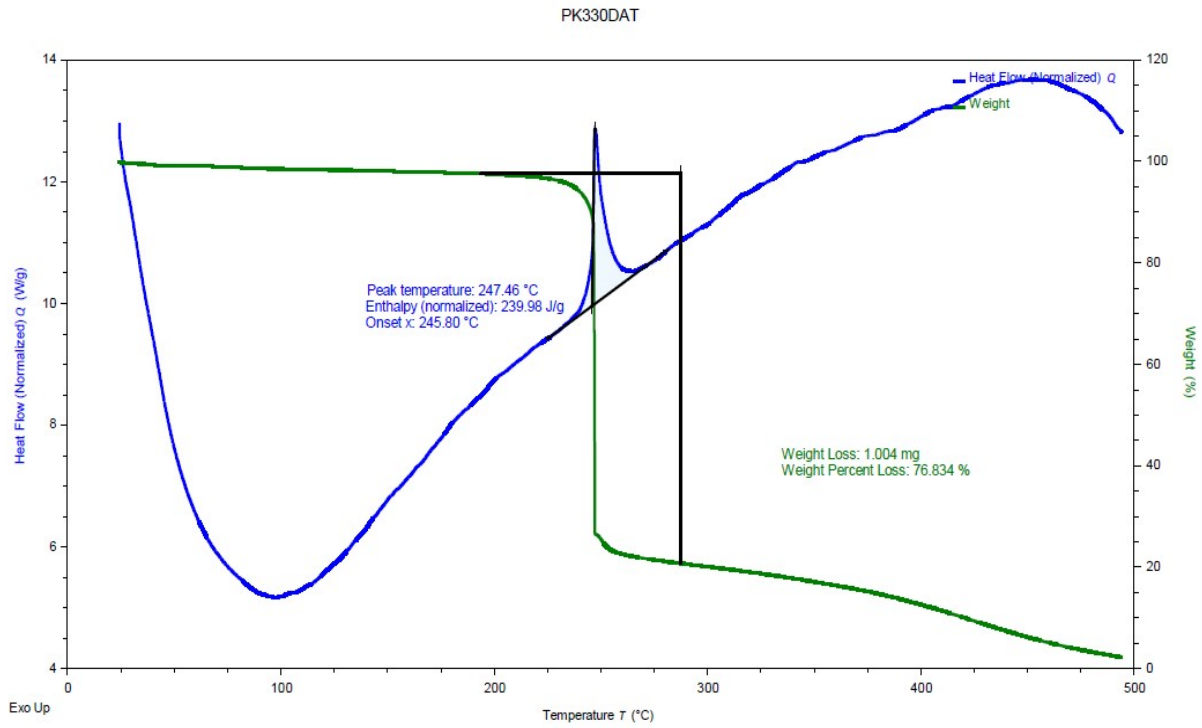

Figure S28: DSC spectrum of compound **7.**

Computational Details:

Computations were carried out using the Gaussian 09 program suite.[2] The structure optimizations are performed with M06-2X/def2-TZVPP level of theory and characterized to be true local energy minima on the potential energy surface and no imaginary frequencies were found. Heat of formation (HOF) is a measure of energy content of an energetic material that can decompose, ignite and explode by heat or impact. It enters into the calculation of explosive and propellant properties such as detonation velocity, detonation pressure, heat of detonation and specific impulse. However, it is impractical to determine the HOF of novel energetic materials because of their unstable intermediates and unknown combustion mechanism. Gas-phase heats of formation for neutral compound and anion were calculated using the isodesmic reaction approach (see **Figure S29**). Calculated total energies and related data for reference compounds and target compounds is listed in Tables S8 and S9. The usage of the HOF_{Gas} in the calculation of detonation properties slightly overestimates the values of

detonation velocity and detonation pressure, and hence, the solid phase HOF (HOF_{Solid}) has been calculated which can efficiently reduce the errors. The HOF_{Solid} is calculated as the difference between HOF_{Gas} and heat of sublimation (HOF_{Sub}) as,

$$HOF_{Solid} = HOF_{Gas} - HOF_{Sub} \quad (1)$$

The heat of sublimation (HOF_{Sub}), which is required to convert the HOF_{Gas} to the HOF_{Solid}, was calculated from Equation (2),[3]

$$HOF_{Sub} = 0.000267\,A^2 + 1.650087\left(v\sigma_{tot}^2\right)^{0.5} - 2.966078 \quad (2)$$

Where A represents the surface area of the 0.001 electrons/bohr^3 isosurface of electronic density, v denotes the degree of balance between the positive and negative surface potentials, and σ_{tot}^2 is the electrostatic potential variance. These molecular surface properties were obtained using the Multiwfn program[4] and listed in Table S10.

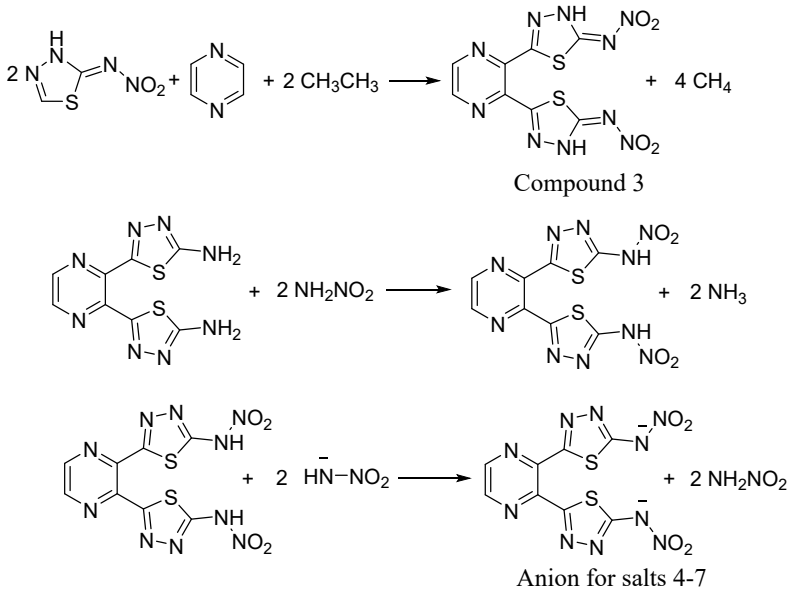

Figure S29. Designed isodesmic reactions for the prediction of gas-phase heats of formation.

Based on the Born–Haber cycle (shown in **Figure S30**), the heat of formation of an ionic compound can be simplified by subtracting the lattice energy of the salt (H_L) from the total heat of formation of salt (see Table S11) *i.e.* sum of the heats of formation of the cation and anion as shown in equation (3).

HOF (salt, 298 K) = HOF (cation, 298 K) + HOF (anion, 298 K) - H_L (3)

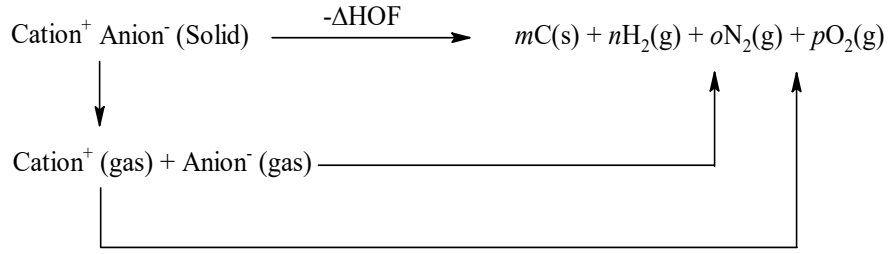

Figure S30. Born-Haber cycle for the formation of energetic salts.

Lattice potential energy is the energy associated with the process in which a crystalline solid lattice, M_pX_q is converted into its constituent gaseous ions, ${}_pM^{q+}$ (g) and ${}_qX^{p-}$ (g). The lattice energy can be predicted with reasonable accuracy by using Jenkins' equation (4).[5]

$$H_L = U_{POT} + [p(\frac{n_M}{2} - 2) + q(\frac{n_X}{2} - 2)]RT \quad (4)$$

where *nM* and *nX* depend on the nature of the ions M_p^+ and X_q^-, respectively, and are equal to 3 for monoatomic ions, 5 for linear polyatomic ions, and 6 for nonlinear polyatomic ions. When lattice potential energy (U_{POT}), is incorporated and made part of a Born–Haber cycle, it needs to be converted into a lattice enthalpy term. This lattice enthalpy (H_L) involves correction of the U_{POT} term by an appropriate number of RT terms.

Table S8. Calculated total energies at 298K (E_0), zero-point energies (ZPE), and thermal corrections (H_T) and experimental HOF_{gas} of reference compounds used isodesmic reaction at the M06-2X/def2-TZVPP level.

Compd.	**E_0 (a.u.)**	**ZPE (au)**	**H_T (au)**	**HOF_{gas} (kJ/mol)**
CH_4	-40.453065	0.0449	0.0038	-74.8
CH_3NO_2	-244.955044	0.0506	0.0053	-81
NH_3	-56.513648	0.0345	0.0038	-45.94
NH_2NO_2	-260.984584	0.0393	0.0042	-6
$NHNO_2$ Anion	-260.458232	0.0271	0.0042	-103.24[a]
CH_3CH_3	-79.727235	0.075	0.0045	-84
CH_3 Anion	-39.782152	0.0285	0.0039	145.14[a]
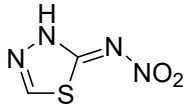	-844.845816	0.0644	0.0080	294.61[a]

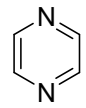	-264.221963	0.0775	0.0051	196.1[a]

[a]Calculated using G4 method.

Table S9. Calculated total energies (E_0), zero-point energies (ZPE), and thermal corrections (H_T) for target compounds at the M06-2X/def2-TZVPP level.

Compd.	E_0 (a.u.)	ZPE (au)	H_T (au)	HOF_{gas}/HOF_{anion} (kJ/mol)	HOF_{Sub} (kJ/mol)
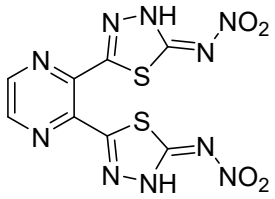	-1951.588289	0.1661	0.0200	831.2	177.3
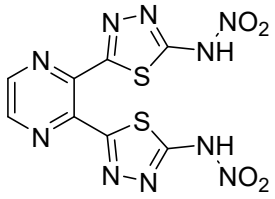	-1951.584511	0.1651	0.0207	740.0	170.1
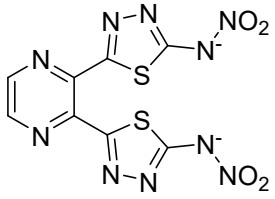	-1950.495365	0.1377	0.0202	641.2	-
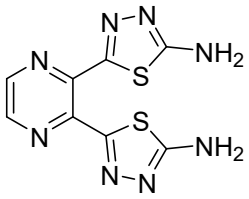	-1542.623754	0.1591	0.0161	709.7	154.1

Table S10. Calculated molecular surface properties of target compounds.

Compd.	Surface area (Å^2)	Volume (Å^3)	σ_{tot}^2 (kcal/mol)	ν
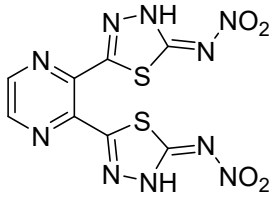	322.39	341.28	199.46	0.2499

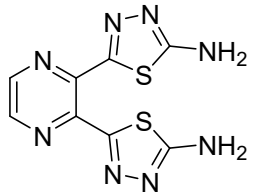	270.90	286.0	298.92	0.2495

Table S11. Energy content of salts 4-7.

Compd.	HOF_c[a]	HOF_a[b]	U_{Pot}[c]	H_L[d]	HOF_{salt}[e]
4	769.5	641.2	1145.70	1158.09	1022.11
5	675.6	641.2	1137.94	1150.33	842.07
6	1112.0	641.2	964.30	976.69	1888.51
7	775.6	641.2	1043.63	1056.02	1136.38

[a]Heat of formation of cation (kJ mol^{-1}). HOF_c data for cations is obtained from Ref. 5. [b]Heat of formation of anion (kJ mol^{-1}). [c]Lattice potential energy (kJ mol^{-1}). [d]Lattice energy (kJ mol^{-1}). [e]Heat of formation of salt (kJ mol^{-1}).

Table S12. Optimized coordinates of compound **2** at M06-2X/def2-TZVPP level of theory.

6	0.704182000	1.322440000	0.007883000
6	-0.704130000	1.322517000	-0.007805000
7	1.375944000	2.463968000	0.114172000
7	-1.375773000	2.464109000	-0.114126000
6	0.687835000	3.595799000	0.091325000
6	-0.687544000	3.595870000	-0.091303000
6	1.514668000	0.108138000	-0.152675000
7	1.203827000	-0.873849000	-0.924432000
16	3.063536000	-0.066508000	0.613679000
7	2.145097000	-1.843741000	-0.975631000
6	3.168538000	-1.577351000	-0.219246000
6	-1.514728000	0.108286000	0.152768000
16	-3.063281000	-0.066589000	-0.614155000
7	-1.204138000	-0.873519000	0.924855000

6	-3.168683000	-1.577120000	0.219292000
7	-2.145471000	-1.843356000	0.976035000
7	4.211579000	-2.447431000	-0.050292000
7	-4.211748000	-2.447171000	0.050311000
1	1.244088000	4.518454000	0.196859000
1	-1.243699000	4.518582000	-0.196853000
1	4.215680000	-3.196115000	-0.726334000
1	5.116177000	-2.050278000	0.137458000
1	-4.216106000	-3.195628000	0.726603000
1	-5.116261000	-2.049995000	-0.137807000

Table S13. Optimized coordinates of compound **3** at M06-2X/def2-TZVPP level of theory.

6	0.700227000	2.145018000	0.055494000
6	-0.700132000	2.145198000	-0.055237000
7	1.361074000	3.288968000	0.202481000
7	-1.360697000	3.289286000	-0.202353000
6	0.682268000	4.421847000	0.134777000
6	-0.681607000	4.422005000	-0.134739000
6	1.558116000	0.953006000	-0.028292000
7	1.274389000	-0.093703000	-0.708701000
16	3.129322000	0.942131000	0.724797000
7	2.281208000	-0.983077000	-0.646204000
6	3.376086000	-0.651932000	0.074120000
6	-1.558246000	0.953345000	0.028619000
16	-3.128692000	0.941844000	-0.726011000
7	-1.275188000	-0.092793000	0.710176000
6	-3.376081000	-0.651706000	-0.074324000
7	-2.281929000	-0.982243000	0.647377000
7	4.494958000	-1.268184000	0.336824000
7	-4.494644000	-1.268217000	-0.337743000
7	4.656336000	-2.525033000	-0.209824000
8	5.690440000	-3.071769000	0.052127000

8	3.774031000	-3.015929000	-0.913492000
7	-4.656494000	-2.524692000	0.209620000
8	-3.774918000	-3.014989000	0.914619000
8	-5.690383000	-3.071597000	-0.052826000
1	1.233285000	5.342338000	0.276114000
1	-1.232391000	5.342622000	-0.276167000
1	2.222564000	-1.869198000	-1.128374000
1	-2.223782000	-1.867954000	1.130361000

Table S14. Optimized coordinates of anionic component for salts **4-7** at M06-2X/def2-TZVPP level of theory.

6	-0.696404000	2.019459000	-0.151213000
6	0.696498000	2.019404000	0.151339000
7	-1.308162000	3.169318000	-0.424449000
7	1.308363000	3.169226000	0.424503000
6	-0.641152000	4.303943000	-0.255697000
6	0.641451000	4.303900000	0.255698000
6	-1.566484000	0.842826000	-0.099037000
7	-1.400488000	-0.139467000	0.727875000
16	-3.056558000	0.760180000	-0.969360000
7	-2.408286000	-1.035386000	0.743486000
6	-3.375687000	-0.735125000	-0.102666000
6	1.566462000	0.842693000	0.099249000
16	3.056585000	0.760010000	0.969486000
7	1.400319000	-0.139729000	-0.727502000
6	3.375424000	-0.735502000	0.103128000
7	2.407961000	-1.035750000	-0.742954000
7	-4.522844000	-1.340101000	-0.476476000
7	4.522132000	-1.341155000	0.477198000
7	5.003271000	-2.328868000	-0.286468000
8	4.539320000	-2.600395000	-1.388808000
8	5.979202000	-2.929217000	0.177006000

7	-5.003257000	-2.329078000	0.286013000
8	-5.980485000	-2.927756000	-0.176941000
8	-4.537354000	-2.603379000	1.386824000
1	-1.155822000	5.225177000	-0.504525000
1	1.156203000	5.225101000	0.504478000

References:

(1) Ghosh, P., Mandal, A. *Green Chemistry Letters and Reviews*, **2011**, *5*, 127–134.

(2) Gaussian 09, Revision E.01, M. J.Frisch, G. W. Trucks, H. B. Schlegel, G. E. Scuseria, M A. Robb, J. R. Cheeseman, G. Scalmani, V. Barone, B. Mennucci, G. A. Petersson, H. Nakatsuji, M Caricato, X. Li, H. P. Hratchian, A. F. Izmaylov, J. Bloino, G. Zheng, J. L. Sonnenberg, M. Hada, M. Ehara, K. Toyota, R. Fukuda, J. Hasegawa, M. Ishida, T. Nakajima, Y. Honda, O. Kitao, H. Nakai, T. Vreven, Jr. J. A. Montgomery, J. E. Peralta, F. Ogliaro, M. Bearpark, J. J. Heyd, E. Brothers, K. N. Kudin, V. N. Staroverov, R. Kobayashi, J. Normand, K. Raghavachari, A. Rendell, J. C. Burant, S. S. Iyengar, J. Tomasi, M. Cossi, N. Rega, J. M. Millam, M. Klene, J. E. Knox, J. B. Cross, V. Bakken, C. Adamo, J. Jaramillo, R. Gomperts, R. E. Stratmann, O. Yazyev, A. J. Austin, R. Cammi, C. Pomelli, J. W. Ochterski, R. L. Martin, K. Morokuma, V. G. Zakrzewski, G. A. Voth, P. Salvador, J. J. Dannenberg, S. Dapprich, A. D. Daniels, O. Farkas, J. B. Foresman, J. V. Ortiz, J. Cioslowski, D. J. Fox, *Gaussian*, Inc., Wallingford CT, **2013**.

(3) Byrd, E. F. C; Rice, B. M.; *J. Phys. Chem. A* **2006**, *110*, 1005-1013.

(4) Lu, T.; Chen, F.; *J. Comput. Chem.* **2012**, *33*, 580.

(5) Jenkins, H. D. B.; Tudela, D.; Glasser, L. *Inorg. Chem.* **2002**, *41*, 2364-2367.